UV-B Perception and Acclimation in *Chlamydomonas reinhardtii*[OPEN]

Kimberley Tilbrook,[a,1] Marine Dubois,[a,2] Carlos D. Crocco,[a] Ruohe Yin,[a] Richard Chappuis,[a] Guillaume Allorent,[a] Emanuel Schmid-Siegert,[b] Michel Goldschmidt-Clermont,[a,c] and Roman Ulm[a,c,3]

[a] Department of Botany and Plant Biology, University of Geneva, Sciences III, CH-1211 Geneva 4, Switzerland
[b] SIB-Swiss Institute of Bioinformatics, University of Lausanne, CH-1015 Lausanne, Switzerland
[c] Institute of Genetics and Genomics of Geneva (iGE3), University of Geneva, CH-1211 Geneva 4, Switzerland

ORCID IDs: 0000-0001-5394-1996 (K.T.); 0000-0003-3579-1829 (M.D.); 0000-0002-6026-4003 (C.D.C.); 0000-0001-6782-4651 (R.Y.); 0000-0003-1339-5120 (E.S.-S.); 0000-0003-1224-5868 (M.G.-C.); 0000-0001-8014-7392 (R.U.)

Plants perceive UV-B, an intrinsic component of sunlight, via a signaling pathway that is mediated by the photoreceptor UV RESISTANCE LOCUS8 (UVR8) and induces UV-B acclimation. To test whether similar UV-B perception mechanisms exist in the evolutionarily distant green alga *Chlamydomonas reinhardtii*, we identified Chlamydomonas orthologs of UVR8 and the key signaling factor CONSTITUTIVELY PHOTOMORPHOGENIC1 (COP1). Cr-UVR8 shares sequence and structural similarity to *Arabidopsis thaliana* UVR8, has conserved tryptophan residues for UV-B photoreception, monomerizes upon UV-B exposure, and interacts with Cr-COP1 in a UV-B-dependent manner. Moreover, Cr-UVR8 can interact with At-COP1 and complement the Arabidopsis *uvr8* mutant, demonstrating that it is a functional UV-B photoreceptor. Chlamydomonas shows apparent UV-B acclimation in colony survival and photosynthetic efficiency assays. UV-B exposure, at low levels that induce acclimation, led to broad changes in the Chlamydomonas transcriptome, including in genes related to photosynthesis. Impaired UV-B-induced activation in the Cr-*COP1* mutant *hit1* indicates that UVR8-COP1 signaling induces transcriptome changes in response to UV-B. Also, *hit1* mutants are impaired in UV-B acclimation. Chlamydomonas UV-B acclimation preserved the photosystem II core proteins D1 and D2 under UV-B stress, which mitigated UV-B-induced photoinhibition. These findings highlight the early evolution of UVR8 photoreceptor signaling in the green lineage to induce UV-B acclimation and protection.

INTRODUCTION

UV-B radiation (280 to 315 nm) accompanies exposure to sunlight and is an abiotic factor that photosynthetic organisms must tolerate. The plant photoreceptor UV RESISTANCE LOCUS8 (UVR8) specifically perceives UV-B via an intrinsic tryptophan-based mechanism, mainly involving Trp-285 and Trp-233 (Rizzini et al., 2011; Christie et al., 2012; Wu et al., 2012). UVR8 is a seven-bladed β-propeller protein that exists as a homodimer maintained by interactions of charged amino acids across the dimer interaction surface (Rizzini et al., 2011; Christie et al., 2012; Wu et al., 2012; Zeng et al., 2015). The charged amino acids that maintain the homodimer are adjacent to the tryptophans involved in photoreception, suggesting that excitation of these tryptophans by UV-B neutralizes dimer-maintaining interactions (Christie et al., 2012; Wu et al., 2012; Mathes et al., 2015).

UV-B activation of UVR8 initiates a molecular signaling cascade leading to UV-B acclimation and the ability to tolerate

constant UV-B exposure (Kliebenstein et al., 2002; Li et al., 2013; Tilbrook et al., 2013; Jenkins, 2014). Briefly, the UVR8 homodimer monomerizes upon UV-B exposure and interacts with CONSTITUTIVELY PHOTOMORPHOGENIC1 (COP1) (Oravecz et al., 2006; Favory et al., 2009; Rizzini et al., 2011). Two separate domains of UVR8 participate in the interaction with COP1: The β-propeller core of UVR8 mediates UV-B-dependent interaction with COP1 and the UVR8 C-terminal C27 domain further stabilizes the interaction and regulates COP1 activity (Cloix et al., 2012; Yin et al., 2015). UVR8-COP1 interaction induces UV-B signaling governed by the bZIP transcription factor ELONGATED HYPOCOTYL5 (HY5) and its homolog HYH (Ulm et al., 2004; Brown and Jenkins, 2008; Stracke et al., 2010; Binkert et al., 2014), which leads to UV-B acclimation (Brown et al., 2005; Oravecz et al., 2006; Favory et al., 2009). The UVR8 UV-B photocycle is completed via the action of negative feedback regulators REPRESSOR OF UV-B PHOTOMORPHOGENESIS1 (RUP1) and RUP2 (Gruber et al., 2010), which directly interact with UVR8 and facilitate redimerization to downregulate UV-B signaling (Heijde and Ulm, 2013; Yin et al., 2015).

The single-celled motile freshwater alga *Chlamydomonas reinhardtii* is a model system for studying photosynthesis, which is useful to complement and extend the understanding of photosynthetic eukaryotes when compared with *Arabidopsis thaliana* (Rochaix, 2002; Gutman and Niyogi, 2004). Chlamydomonas is a photoautotrophic organism in the wild and is exposed to a complex light environment that includes UV-B. When found

in aqueous habitats, Chlamydomonas UV-B exposure is expected to be less than that of sunlight-exposed land plants, as UV-B attenuates rapidly in the water column. The depth of UV-B penetration depends on the amount of dissolved or suspended UV-B-absorbing compounds present and thus can vary from within a few centimeters to a few meters of freshwater surfaces (Hader, 2000). Other motile aquatic organisms, such as *Euglena gracilis*, migrate throughout the water column using a combination of gravitaxis and phototaxis to select an optimal position for photoautotrophic growth while avoiding potential light stress (Richter et al., 2007). Phototaxis is also a well characterized feature of Chlamydomonas (Kateriya et al., 2004). However, while Chlamydomonas may exhibit mobile UV-B avoidance strategies, a compromise must still be made regarding UV-B exposure in the water column to ensure that the cells intercept adequate photosynthetically active radiation. Also, physical UV-B protection in the water column does not contribute toward survival of Chlamydomonas in damp soil, an environment from which the Chlamydomonas wild-type laboratory strains have been isolated (Harris, 2009). It can be assumed that in stagnant water or on damp soil, Chlamydomonas UV-B exposure would be comparable to levels that land plants can tolerate via engagement of the UVR8 UV-B signaling pathway.

Like higher plants, Chlamydomonas makes use of a sophisticated photoreceptor network to monitor the light environment and regulate cellular processes in response to changes in light intensity, direction, and quality (Kianianmomeni and Hallmann, 2014). Specifically, Chlamydomonas possesses a single phototropin (Huang and Beck, 2003), rhodopsins, including channelrhodopsins (Nagel et al., 2002, 2003; Kateriya et al., 2004), a plant-like cryptochrome (Reisdorph and Small, 2004), and an animal-like cryptochrome that responds to both blue and red light (Beel et al., 2012). Furthermore, a histidine kinase rhodopsin was recently characterized that exists in both UV-A- and blue-light-absorbing isoforms (Luck et al., 2012). No phytochromes can be found in the Chlamydomonas genome, leading to speculation that the observed red- and far-red-light responses in the organism are controlled by other photoreceptors in a manner that differs from phytochrome regulation in higher plants (Kianianmomeni and Hallmann, 2014).

Arguably, all sun-exposed organisms require a means of UV-B protection, and initial evolutionary analysis revealed good conservation of UVR8 in the plant lineage (Rizzini et al., 2011). We set out to establish if evolutionary conserved UVR8-dependent UV-B signaling existed in Chlamydomonas. Here, we show that UV-B acclimation occurs in Chlamydomonas and a conserved UVR8 UV-B photoreceptor is present that monomerizes under UV-B and interacts with Chlamydomonas COP1. Mutation of *Cr-COP1* in the Chlamydomonas *hit1* strain results in impaired UV-B responses and acclimation. When expressed in Arabidopsis *uvr8* null mutants, Cr-UVR8 is able to restore UV-B perception and signaling. We also explore the link between UV-B acclimation, the levels of PSII proteins D1 and D2, and photosynthesis.

RESULTS

Structural Conservation and UV-B Dynamics of Chlamydomonas UVR8

The presence of a Chlamydomonas UVR8-like UV-B photoreceptor was proposed previously (Rizzini et al., 2011) based on its identification in the Chlamydomonas genome sequence (Merchant et al., 2007). However, the available sequence annotation at the time indicated that the putative Cr-*UVR8* encoded a UVR8-like protein missing the C-terminal portion, including the C27 domain (Rizzini et al., 2011). For this work, we queried the predicted Chlamydomonas proteome (Phytozome v10) with Arabidopsis UVR8 (herein referred to as At-UVR8) in conjunction with analysis of the At-UVR8 Gene Homologs resource on Phytozome (http://phytozome.jgi.doe.gov), which allowed us to identify Cre05.g230600 as the likely candidate for Chlamydomonas UVR8 (herein referred to as Cr-UVR8). Cr-UVR8 was found to possess a similar sequence length (465 amino acids versus 440 amino acids for At-UVR8) and the same domain profile as At-UVR8, including the C27 domain (Figure 1). This indicated that the annotated coding sequence in the initial genome release was incorrect and Chlamydomonas possesses a full-length UVR8-like protein. Alignment of At-UVR8 and Cr-UVR8 revealed high pairwise sequence identity of over 45% (Supplemental Figure 1). Greater sequence conservation was observed surrounding most tryptophan residues, including those of the tryptophan triad (highly conserved GWRHT/S motif of W233, W285, and W337 in At-UVR8; Tilbrook et al., 2013) (Figure 1A; Supplemental Figure 1). Comparable positioning of RCC1 (PF00415) domains was also observed in both At-UVR8 and Cr-UVR8 (Figure 1A). Indeed, structural modeling of Cr-UVR8 suggests the protein has a β-propeller structure similar to At-UVR8 (Figure 1C). Most importantly, modeling predicted a comparable localization of tryptophans at the homodimeric interface of both proteins, and Cr-UVR8 was shown to have equivalent residues to At-UVR8 W285 and W233 (Figure 1C). Also apparent was good conservation of the charged amino acids that facilitate electrostatic interactions across the dimer interaction surface in At-UVR8 (Supplemental Figure 1). This notably includes the potential for interactions of R282 (*R286* in At-UVR8) with D91 (*D96*) and D102 (*D107*), and R346 (*R338*) with E38 (*E43*) and D39 (*D44*), which are particularly important in maintaining the At-UVR8 homodimer (Christie et al., 2012; Wu et al., 2012). Moreover, the C27 domain of At-UVR8 is conserved in Cr-UVR8 (Figure 1B; Supplemental Figure 1), including the Val-Pro pair (Val^{420}-Pro^{421} in Cr-UVR8; Val^{410}-Pro^{411} in At-UVR8) important for interaction of At-UVR8 with AtCOP1 (Yin et al., 2015).

To analyze the Cr-UVR8 protein, we generated an anti-CrUVR8 antibody against an N-terminal peptide (Cr-UVR8$^{34-49}$). Cr-UVR8 was detected as two distinct bands in immunoblots of nonboiled protein extracts of Chlamydomonas grown in the absence of UV-B (Figure 1D). As previously established for At-UVR8 (Rizzini et al., 2011), the larger of these two bands was only visible when the protein extracts were left unboiled prior to gel electrophoresis and the gel itself was UV-B irradiated (Figure 1D). Based on the previously described properties of
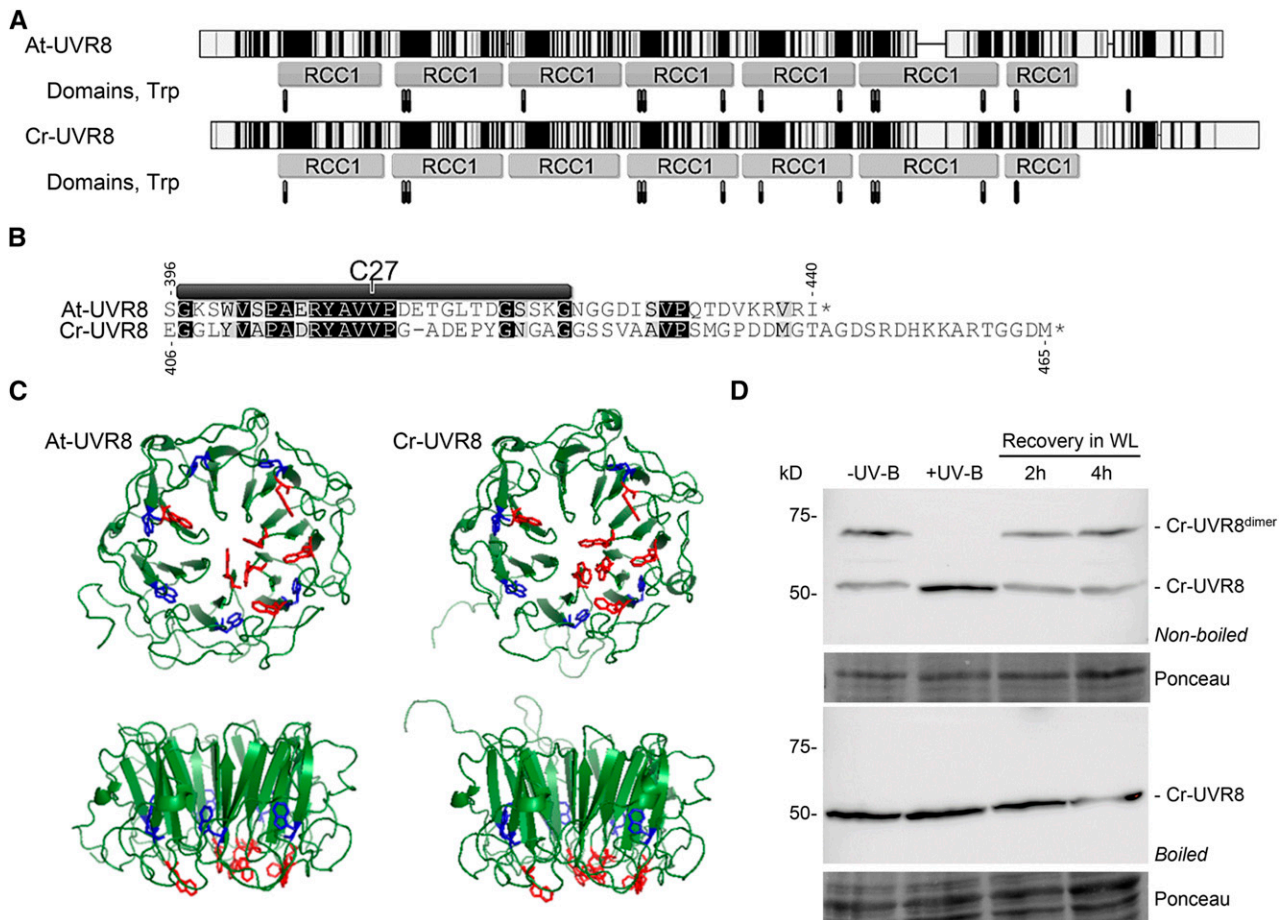
Figure 1. Chlamydomonas Has an At-UVR8 Ortholog, Which Is UV-B Responsive.

(A) Protein sequence alignment of At-UVR8 with Cr-UVR8 with identical aligned residues highlighted in black and similar and nonsimilar residues highlighted in gray and white, respectively. Positioning of RCC1 domains and tryptophan residues are also indicated.

(B) Protein sequence alignment of At-UVR8 and Cr-UVR8 C termini, with location of the C27 region of At-UVR8 indicated.

(C) At-UVR8 structure (left) and predicted structural model of Cr-UVR8 (right), each depicting a single monomer viewed from the dimeric interaction surface (upper images) and from the side (lower images). Tryptophan residues are highlighted in blue for those located in the β-propeller blades and in red for those located in the dimer interaction surface.

(D) Cr-UVR8 monomerization in response to UV-B and subsequent redimerization in the absence of UV-B. Chlamydomonas cells were irradiated for 30 min with broadband UV-B before recovery in white light (WL) for the indicated times. Cr-UVR8 dimers were detectable in nonboiled protein samples, as described previously for At-UVR8 (Rizzini et al., 2011). Parallel boiled samples demonstrated equal amounts of Cr-UVR8 protein and Ponceau staining of membranes equal protein loading between lanes.

non-heat-denatured At-UVR8 in SDS-PAGE (Rizzini et al., 2011) and conservation of the key residues known to maintain At-UVR8 homodimers in Cr-UVR8, the upper band very likely represents the Cr-UVR8 homodimer and the lower band represents the Cr-UVR8 monomer (Figure 1D). It should be noted, however, that this upper band corresponds to a lower molecular mass than the predicted 96.4 kD for the denatured Cr-UVR8 homodimer (predicted Cr-UVR8 monomer: 48.2 kD). However, analogous aberrant migration of non-heat-denatured At-UVR8 homodimers is well documented (Rizzini et al., 2011) and most importantly is also observed with purified homodimeric recombinant At-UVR8 (Christie et al., 2012; Heilmann and Jenkins, 2013). In agreement, only the lower band corresponding to the

Cr-UVR8 monomer was detected upon UV-B irradiation of Chlamydomonas, and in a higher amount (Figure 1D). This suggested Cr-UVR8 monomer accumulation due to monomerization of the Cr-UVR8 dimer, confirming that Cr-UVR8 is UV-B responsive in vivo. Cr-UVR8 dimer was restored following recovery of cells in white light devoid of UV-B (Figure 1D), in agreement with known redimerization of At-UVR8 (Heijde and Ulm, 2013; Heilmann and Jenkins, 2013). Thus, we conclude that Cr-UVR8 is likely a homodimer in the absence of UV-B and that Cr-UVR8 monomerizes in response to UV-B in Chlamydomonas. This is further supported by the highly conserved structure of Cr-UVR8 and the well-established properties of the At-UVR8 photoreceptor in Arabidopsis.

Cr-UVR8 Interacts with Cr-COP1 in a UV-B-Dependent Manner in Yeast

In the same manner that Cr-UVR8 was identified, the putative ortholog of Arabidopsis At-COP1 was identified as Cre02. g085050 (herein referred to as Cr-COP1; previously also described as PUTATIVE LIGHT RESPONSE SIGNALING PROTEIN1 [LRS1]; Schierenbeck et al., 2015). The identification of Cr-COP1 further suggests the presence of a conserved UV-B signaling pathway similar to the known pathway in Arabidopsis (Heijde and Ulm, 2012; Li et al., 2013; Tilbrook et al., 2013; Jenkins, 2014). Cr-*UVR8* and Cr-*COP1* cDNAs were cloned and verified to match their respective sequence annotations. Of note, Cr-COP1 (1443 amino acids) is more than twice as large as At-COP1 (675 amino acids) but possesses the same functional domains and good conservation of protein sequence corresponding to RING, coiled-coil, and WD40-repeat domains (Figure 2).

In a yeast two-hybrid assay, Cr-UVR8 interacted with Cr-COP1 and At-COP1 specifically under UV-B (Figure 2B), mimicking the UV-B-dependent interaction previously observed between At-UVR8 and At-COP1 (Rizzini et al., 2011; Cloix et al., 2012; O'Hara and Jenkins, 2012; Heijde et al., 2013; Huang et al., 2014; Yin et al., 2015). This suggests that a UVR8 photocycle exists in Chlamydomonas (Figure 2C) that is very similar to what has been demonstrated in Arabidopsis (Tilbrook et al., 2013).

Cr-UVR8 Complements the Arabidopsis *uvr8* Null Mutant

A Cr-*UVR8* cDNA driven by the CaMV 35S promoter was introduced into the Arabidopsis *uvr8-6* null mutant (herein referred to as *uvr8*). Multiple independent transgenic lines were generated with Cr-*UVR8* (Figure 3) and Cr-*UVR8* fused with CFP (both CFP-Cr-UVR8 and Cr-UVR8-CFP, predicted molecular mass of 76.3 kD; Supplemental Figure 2), which were detected at the protein level using the anti-CrUVR8[34-49] antibodies. Cr-UVR8 was detected only in transformed *uvr8* lines and at a size expected from its predicted molecular mass (48.2 kD; Figure 3A). In all transgenic lines tested, restored UV-B perception and signaling was shown using known markers as output of the UVR8 UV-B signaling pathway. *HY5* and *CHALCONE SYNTHASE* (*CHS*) gene activation under UV-B, which is observed in the wild type but absent in *uvr8*, was restored in *uvr8* lines complemented with either Cr-UVR8 or Cr-UVR8 fused with CFP (Figures 3B and 3C; Supplemental Figures 2B and 2C). Similarly, CHS protein accumulation in response to UV-B, a normal response of the wild type but absent in *uvr8* mutants, was present in complemented lines (Figure 3D; Supplemental Figure 2D). Finally, complementation of *uvr8* with either Cr-UVR8 or Cr-UVR8 fused with CFP restored UV-B-induced inhibition of hypocotyl growth, which is not seen in *uvr8* seedlings (Figures 3E and 3F; Supplemental Figures 2E and 2F). The complementation of *uvr8* confirmed that Cr-UVR8 is similar enough to At-UVR8 to seamlessly restore UV-B perception and signaling in Arabidopsis and thus is a bona fide UV-B photoreceptor.

UV-B Exposure Induces UV-B Acclimation and Stress Tolerance in Chlamydomonas

With Cr-UVR8 established as a UV-B photoreceptor capable of initiating a UV-B signaling pathway, further investigation was conducted to address the in vivo UV-B responses in Chlamydomonas. Low-level narrowband UV-B exposure was seen to affect Chlamydomonas in that the rapid increase in cell density during the exponential phase of liquid culture growth was delayed, but ultimately +UV-B cultures reached a similar stationary phase cell density as those cultures shielded from UV-B (Supplemental Figure 3). We further tested whether a diluted "+UV-B culture" is less affected by UV-B than a naïve culture. However, the UV-B effect on growth was maintained in subsequent liquid cultures, even when inoculated with cells prior exposed to UV-B (Supplemental Figure 3B), indicating that daughter cells of UV-B-exposed Chlamydomonas were also affected by continuing exposure.

We used these irradiation conditions to test whether Chlamydomonas is able to acclimate to UV-B, similar to the UVR8-dependent acclimation response known in Arabidopsis (Favory et al., 2009; González Besteiro et al., 2011). Indeed, continuous low-level narrowband UV-B exposure of Chlamydomonas was seen to improve tolerance and survival under subsequent broadband UV-B stress treatment (Figure 4). This process of UV-B acclimation was demonstrated by assessing the survival of Chlamydomonas colonies subjected to broadband UV-B stress, comparing colonies previously grown under supplemental low-level narrowband UV-B versus colonies grown with no prior exposure to UV-B. Broadband UV-B stress resulted in a reduced number of surviving colonies for those pregrown under nonacclimating conditions, whereas a significantly greater survival rate was observed in acclimated colonies (Figure 4A, "Acclimated" versus "Non-acclimated").

We further tested whether UV-B acclimation is also apparent when focusing on photosynthesis and the damage inflicted to PSII by broadband UV-B. We first established that under our conditions broadband UV-B stress indeed impacted photosynthetic efficiency by decreasing the maximum quantum yield of PSII as determined by chlorophyll fluorescence spectroscopy (Fv/Fm) (Figure 4B, "Non-acclimated"). Decreased photosynthetic efficiency due to light-induced damage is generally referred to as photoinhibition (Hakala-Yatkin et al., 2010). The extent of UV-B-induced photoinhibition increased with broadband UV-B treatment time (Figure 4B). However, UV-B acclimated cells previously grown under low-level narrowband UV-B displayed less UV-B-induced photoinhibition following broadband UV-B stress than non-acclimated cultures (Figure 4B). It is of note that supplemental narrowband UV-B had no detrimental effect of its own regarding both colony survival and UV-B-induced photo-inhibition in control samples not treated with broadband UV-B ($-$UV-B) (Figure 4). We thus conclude that in Chlamydomonas, low-level narrowband UV-B treatment results in UV-B acclimation and stress tolerance resembling the UVR8-mediated acclimation response in Arabidopsis.
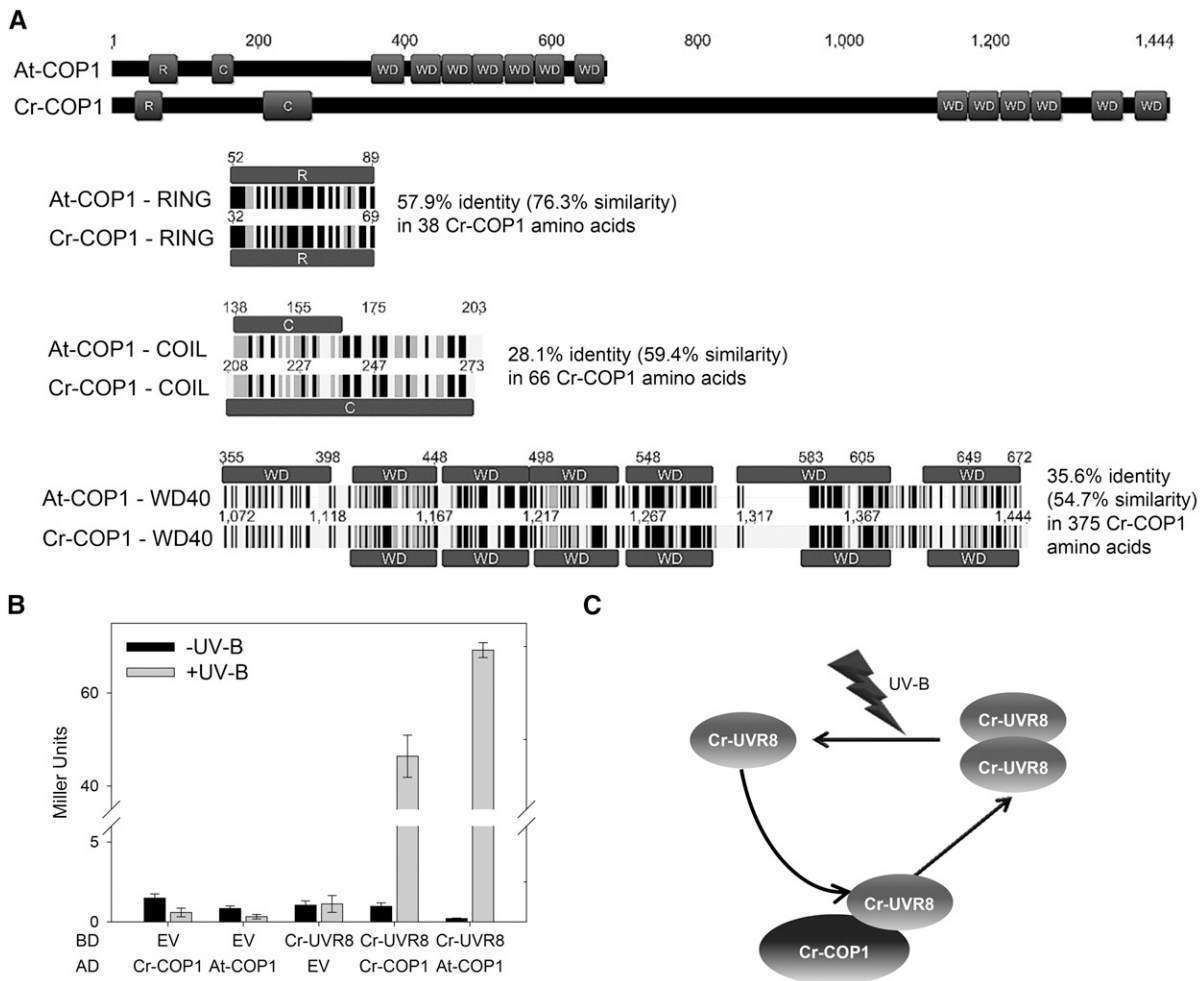
Figure 2. Chlamydomonas Has an At-COP1 Ortholog, Which Interacts UV-B-Dependently with Cr-UVR8.

(A) Top: Schematic protein comparison of At-COP1 with Cr-COP1 showing identity and layout of protein domains. Bottom: Protein sequence alignment of individual RING, coiled-coil, and WD40 domains within At-COP1 and Cr-COP1. Identical aligned residues highlighted in black and similar and nonsimilar residues highlighted in gray and white, respectively.

(B) Quantitative yeast two-hybrid assays were performed in the presence or absence of UV-B. Miller units represent β-galactosidase activity. AD, activation domain construct; BD, binding domain construct; EV, empty vector. Means and se are shown (*n* = 3).

(C) Working model of the Cr-UVR8 UV-B photocycle. Cr-UVR8 exists as a homodimer that monomerizes upon UV-B exposure and interacts with Cr-COP1. In the absence of UV-B, Cr-UVR8 homodimer reforms, thus completing the UV-B photocycle.

UV-B Acclimation in Chlamydomonas Maintains D1 and D2 Protein Levels under High-Level UV-B

Chlamydomonas UV-B acclimation preserves photosynthetic efficiency upon UV-B treatment that causes photoinhibition (Figure 4B). The PSII protein complex, with D1 and D2 at its core, is susceptible to photodamage leading to photoinhibition, particularly by UV-B (Takahashi et al., 2010). Photoinhibition is closely linked to the turnover of D1 and, to a lesser extent, D2 during such photodamage (Schuster et al., 1988). Thus we investigated UV-B acclimation at the molecular level by measuring levels of the PSII core proteins D1 and D2 (Figure 5). In agreement with UV-B-induced photoinhibition, levels of D1 and D2 were reduced following broadband UV-B stress

(Figures 5A to 5D; "−CAM", "Non-acclimated"). However, in acclimated cells, D1 and D2 levels decreased less following broadband UV-B stress (Figures 5A to 5D; "−CAM", "Acclimated"). We then investigated whether the protective effect of UV-B acclimation on D1 and D2 protein levels was due to regeneration of damaged components of the photosynthetic apparatus. For this, the UV-B acclimation experiments were repeated but chloramphenicol (CAM) was added during the broadband UV-B stress. A 30-min incubation with 100 µg/mL CAM was deemed sufficient to inhibit chloroplast translation (Supplemental Figure 4). Greater UV-B-induced photoinhibition, indicating a lack of chloroplast translation and PSII subunit resynthesis, was observed after ~20 min in Chlamydomonas cultures treated with CAM compared with
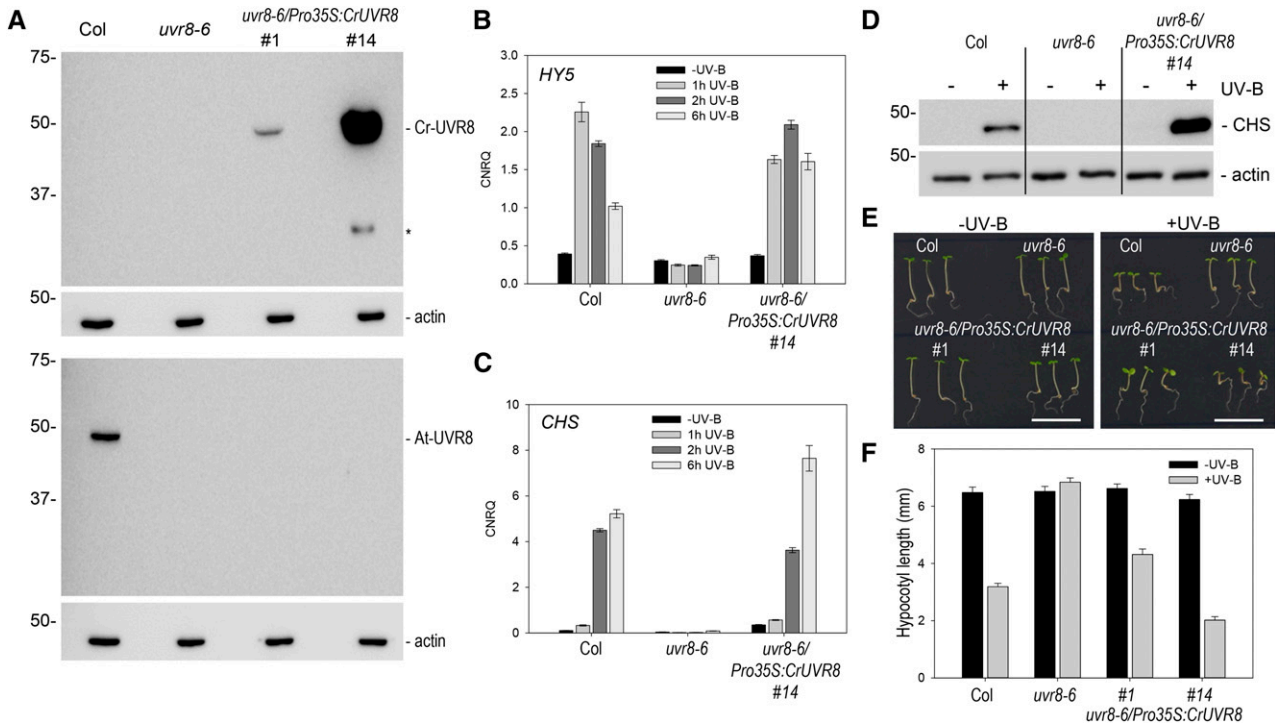
Figure 3. Transgenic Expression of Cr-*UVR8* in Arabidopsis Complements the *uvr8* Mutant UV-B Phenotype.

(A) Presence of Cr-UVR8 or At-UVR8 in wild-type (Col), *uvr8-6* mutant, and complemented (*uvr8-6/Pro35S:CrUVR8*) Arabidopsis lines. Top, anti-CrUVR8 immunoblot; bottom, anti-AtUVR8 immunoblot. Actin immunoblots show individual lane protein loading. Asterisk indicates a degradation product.
(B) and **(C)** UV-B-dependent induction of **(B)** *HY5* and **(C)** *CHS* UV-B marker genes. CNRQ, calibrated normalized relative quantities. Means and se are shown (*n* = 3).
**(D)** UV-B-dependent CHS protein accumulation. Actin is shown as protein loading control.
(E) and **(F)** UV-B-induced hypocotyl growth inhibition. Images of representative individuals (bar = 1 cm) **(E)** and quantification of hypocotyl lengths **(F)** of 4-d-old seedlings grown under white light with (+UV-B) or without (−UV-B) supplementary UV-B light. Means and se are shown (*n* = 15).

nontreated controls (Supplemental Figure 4). Maintenance of D1 and D2 following UV-B acclimation thus depended on chloroplast translation as the addition of CAM equalized the effect that broadband UV-B stress had on nonacclimated and acclimated culture cells, with equal and larger reduction in D1 and D2 levels observed for both (Figures 5A to 5D; "+CAM", "Non-acclimated" versus "Acclimated"). The dynamics of D1 and D2 protein levels in these experiments were consistent with UV-B-induced photoinhibition monitored by measuring Fv/Fm in the UV-B acclimation assay. As presented above, less UV-B-induced photoinhibition was observed in UV-B acclimated culture cells following broadband UV-B stress (Figure 5E). In the absence of UV-B stress, the presence of CAM alone did not appear to affect photosynthetic efficiency in either nonacclimated or acclimated cells over the course of CAM treatment. However, the combination of CAM and broadband UV-B stress resulted in equal and drastic UV-B-induced photoinhibition in both nonacclimated and acclimated culture cells, and the UV-B acclimation effect seen in the control experiment was no longer apparent (Figure 5E). We conclude that UV-B acclimation in Chlamydomonas alleviates subsequent UV-B-induced photoinhibition and is associated with the induction of faster rates of D1 and D2 resynthesis.

UV-B Exposure at Acclimation-Inducing Levels Causes Global Changes in Gene Expression

As UV-B acclimation was evident in Chlamydomonas, we were thus interested in characterizing the genes regulated by UV-B exposure at acclimation-inducing levels. One-hour exposure of Chlamydomonas cells growing in liquid culture to low-level narrowband UV-B was accompanied by broad changes in gene expression, as determined by RNA-seq (Figure 6). With a 5% false discovery rate (FDR) and a 2-fold change threshold applied ($|\log_2 FC| \geq 1$), a total of 2601 genes were seen to vary in expression upon UV-B exposure, with a fairly equal distribution of 1326 genes upregulated and 1275 genes downregulated in response to UV-B (Figure 6A; Supplemental Data Set 1). A set of five upregulated and four downregulated genes across a wide range of fold-change expression were selected as marker genes for the Chlamydomonas response to acclimation-inducing low-level narrowband UV-B. The magnitudes of expression change of these nine genes in response to UV-B were confirmed using RT-qPCR (Figure 6B), supporting the quality of the RNA-seq data. It is of note that among the confirmed upregulated genes there are two that we identified as putative orthologs of the Arabidopsis genes *HY5* (Cre06.g310500) and *RUP1/RUP2* (Cre01.g053850) (Figure 6B;
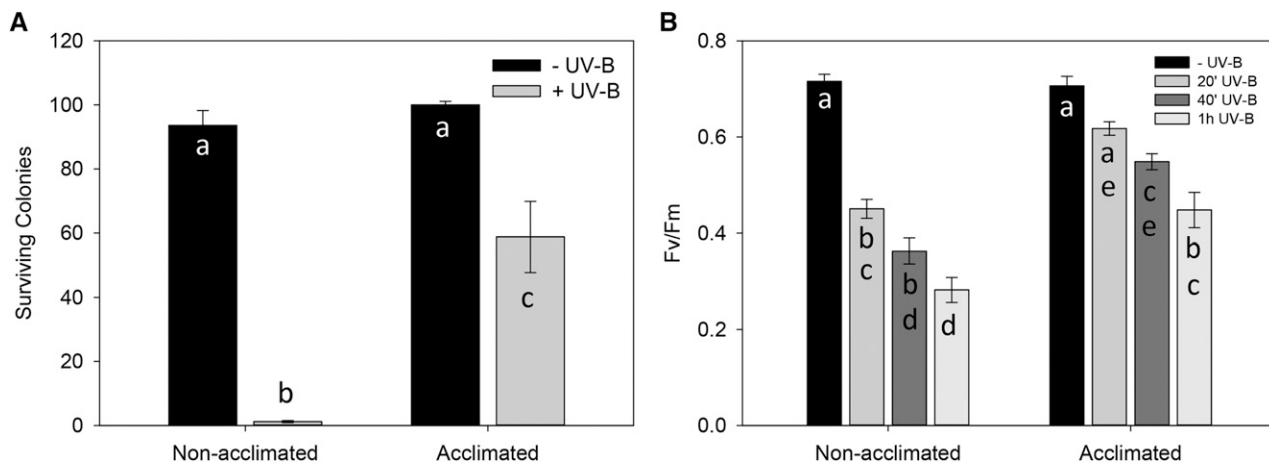
Figure 4. Chlamydomonas Acclimates to UV-B, Resulting in Elevated UV-B Stress Tolerance.

(A) Survival of Chlamydomonas UV-B acclimated and nonacclimated colonies following broadband UV-B stress. –UV-B, no broadband UV-B stress; +UV-B: 4 h broadband UV-B stress exposure. Means and SE are shown ($n = 5$). Shared letters indicate no statistically significant difference in the means (P > 0.05).
(B) UV-B-induced photoinhibition in Chlamydomonas as measured by a reduction of the chlorophyll fluorescence parameter Fv/Fm following broadband UV-B stress. Means and SE are shown ($n = 3$). –UV-B, no broadband UV-B stress; 20'/40'/1 h UV-B, duration of broadband UV-B stress exposure; Non-acclimated, grown under weak white light only; Acclimated, grown under equivalent white light supplemented with narrowband UV-B. Shared letters indicate no statistically significant difference in the means (P > 0.05).

Supplemental Data Set 1). *HY5*, *RUP1*, and *RUP2* are UV-B-induced genes in Arabidopsis as well and play important roles in UV-B signaling (Ulm et al., 2004; Brown et al., 2005; Gruber et al., 2010; Heijde and Ulm, 2013). Independent of this, among all the UV-B-induced genes, 24 were found to be induced over 10-fold by UV-B. Interestingly, many of them are light-harvesting complex (LHC)-like members of the chlorophyll *a/b* binding family (Table 1). This suggests that UV-B acclimation may involve protection of the photosynthetic apparatus using a broad range of LHC-like proteins.

It is of note that a significant number of genes we report as differentially expressed in response to acclimatory UV-B have been previously identified as differentially expressed within 30 min when Chlamydomonas cells were transferred from dark to white light (Duanmu et al., 2013) (Supplemental Figure 5). Similar to supplemental UV-B exposure, the transition from darkness to white light may result in an acclimatory response that, among other processes, promotes protection of the photosynthetic machinery. Indeed, of the 1326 UV-B-induced and 1275 UV-B-repressed genes that could be compared with the dark-to-white-light data set, >29% (388) and >24% (312), respectively, were found to be common to both light transitions (Supplemental Figure 5 and genes listed in Supplemental Data Sets 2 and 3). Within these comparisons, it is most apparent that the commonly induced genes encompass those encoding proteins that can be associated with photosynthesis and photoprotection (including *PSBS1*, *PSBS2*, *LHCSR1*, *LHCSR3.1*, *LHCSR3.2*, and *ELI1*).

### Cr-COP1 Is Required for UV-B-Induced Responses and Acclimation in Chlamydomonas

The *high light tolerant1* (*hit1*) mutant was recently described containing a mutation replacing Arg-1256 with Pro in the

WD40-repeat domain of Cre02.g085050 (Schierenbeck et al., 2015), thus representing a putative *Cr-COP1* mutant strain. Interestingly, in contrast to the enhanced UV-B tolerance that was seen to evolve in the wild type, a lesser survival rate in response to UV-B stress was observed in UV-B-acclimated *hit1* colonies (Figure 7A). Moreover, higher maintenance of D1 following UV-B stress of acclimated cells seen for the wild type was not observed in *hit1* cultures (Figure 7B). Furthermore, comparison of UV-B-induced photoinhibition following broadband UV-B stress in the wild type and *hit1* showed that prior exposure to low-level narrowband UV-B did not reduce UV-B-induced photoinhibition in *hit1* (Figure 7C). Finally, the *hit1* strain was impaired in UV-B-induced expression changes of several tested marker genes (Figure 7D). These results all imply that the Cr-*COP1* mutation in *hit1* impaired its ability to respond and acclimate to UV-B. The *hit1* strain was then complemented with wild-type Cr-*COP1* under expression control of the *psaD* promoter (*hit1/Pro_psaD:CrCOP1*). This restored a resistance to UV-B-induced photoinhibition after acclimation (Figure 7C), as well as most UV-B-induced expression changes (Figure 7D). These results confirmed that the absence of UV-B responses and acclimation in the *hit1* strain is indeed due to a mutation in the Cr-*COP1* gene.

DISCUSSION

The UVR8-COP1 UV-B Perception and Signaling Pathway in Chlamydomonas

When considering the well established features of UVR8-UV-B signaling in Arabidopsis, our results indicate that Chlamydomonas has an analogous UV-B signaling pathway governed by Cr-UVR8. Importantly, Cr-UVR8 contains conserved key tryptophans
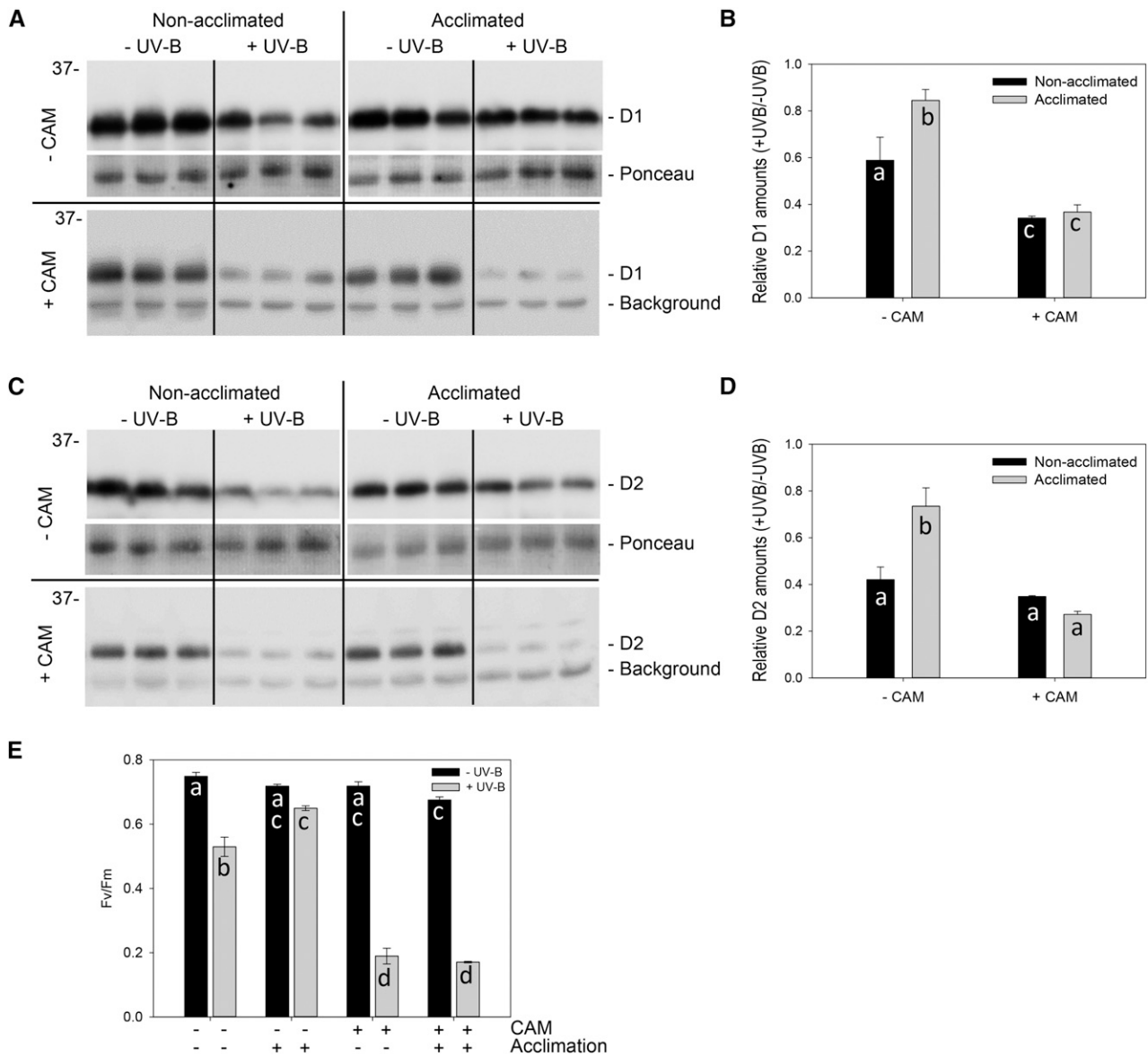
Figure 5. Chlamydomonas UV-B Acclimation to Maintain Photosynthetic Efficiency Is Associated with Regeneration of D1 and D2 Proteins and Is Dependent on Chloroplast Translation.

(A) Immunoblot analysis of D1 protein level in triplicate replicate cultures of UV-B-acclimated or nonacclimated Chlamydomonas before (−UV-B) and following (+UV-B) broadband UV-B stress. Replicate experiments are shown performed in the presence or absence of the chloroplast translation inhibitor CAM (+CAM and −CAM, respectively).
**(B)** Quantification of D1 protein levels shown in **(A)**. Depicted are protein levels from broadband UV-B-treated samples (+UV-B) relative to protein levels in untreated controls (−UV-B). Means and sᴇ are shown (*n* = 3). Shared letters indicate no statistically significant difference in the means (P > 0.05).
(C) As for **(A)** but for D2 protein.
(D) As for **(B)** but for D2 protein.
(E) UV-B-induced photoinhibition in Chlamydomonas as measured by a decrease of the maximum quantum yield of PSII (Fv/Fm) following broadband UV-B stress. Replicate experiments are shown performed in the presence or absence of CAM. –UV-B, no broadband UV-B; + UV-B, 1 h broadband UV-B exposure; Non-acclimated, grown under low-level PAR only; Acclimated, grown under equivalent PAR supplemented with narrowband UV-B. Means and sᴇ are shown (*n* = 3). Shared letters indicate no statistically significant difference in the means (P > 0.05).
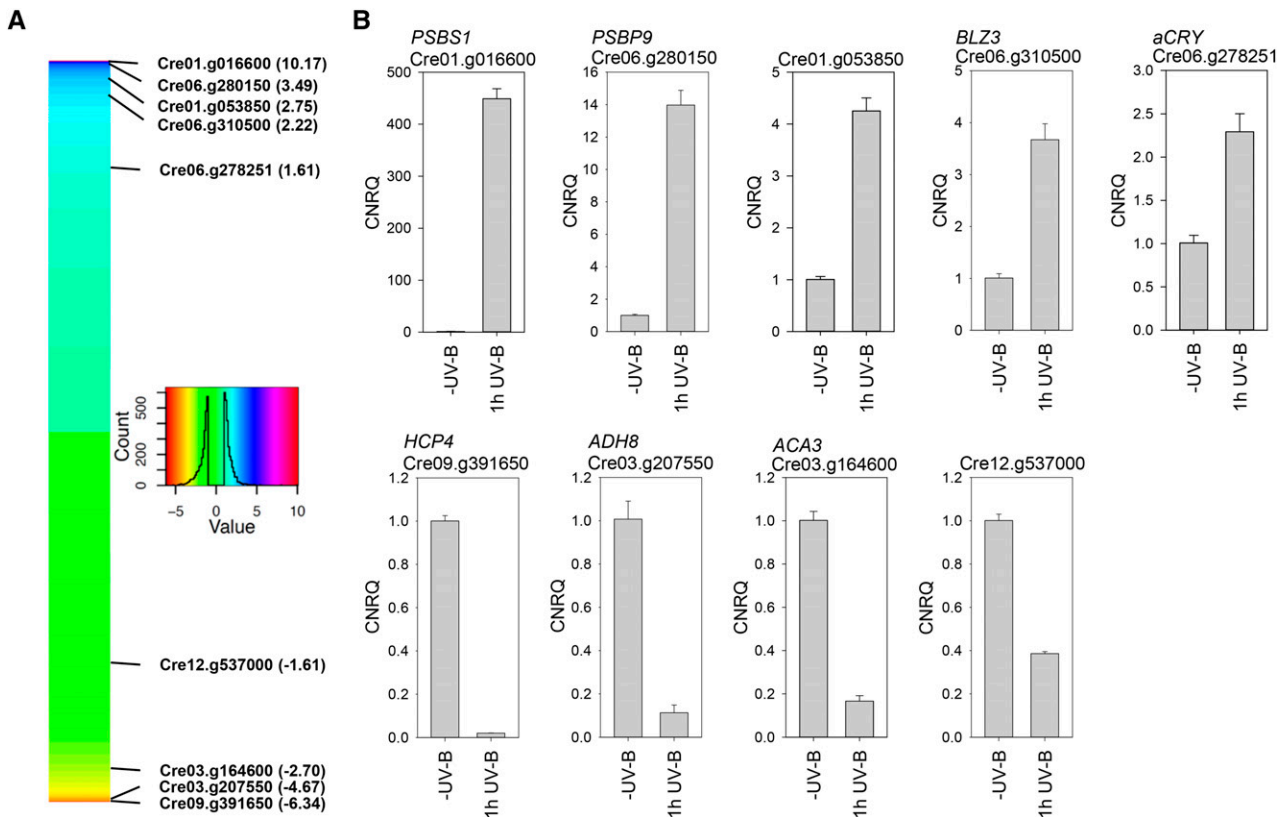
Figure 6. Narrowband UV-B Induces Global Gene Expression Changes in Chlamydomonas.

(A) Heat map of gene expression changes in Chlamydomonas exposed to 1 h narrowband UV-B with a cutoff of more than 2-fold change ($\log_2$ FC $\geq$ 1) applied. Positioning of genes selected for RT-qPCR validation of expression changes are indicated with gene identifiers and their $\log_2$ fold change in expression (bracketed).

(B) Individual RT-qPCR analysis of select Chlamydomonas genes. Expression of each gene following 1 h UV-B is normalized to levels in minus UV-B control samples. CNRQ, calibrated normalized relative quantities.

for UV-B perception, as well as corresponding residues of crucial importance for stable homodimerization of At-UVR8 in the absence of UV-B. Moreover, Cr-UVR8 is detected as two bands in non-heat-denatured protein samples of Chlamydomonas grown in the absence of UV-B, one at the expected size of the Cr-UVR8 monomer and one slower migrating band. Even though we presently cannot formally exclude that the slower migrating form of Cr-UVR8 represents a heterodimer with an unknown interaction partner that is released upon UV-B treatment, we suggest that this band represents homodimeric Cr-UVR8. This is despite the fact that the band migrates at a lower apparent molecular mass than is expected for the denatured Cr-UVR8 homodimer. Such band patterns have been previously extensively described, including for highly purified recombinant homodimeric At-UVR8 (Rizzini et al., 2011; Christie et al., 2012; Heilmann and Jenkins, 2013). Thus, there is substantial evidence that Cr-UVR8, like At-UVR8, is homodimeric in the absence of UV-B. Independent of this, Cr-UVR8 was shown to monomerize in response to UV-B, to interact UV-B-dependently with Cr-COP1 and At-COP1 in yeast, and to functionally complement UV-B perception and response when expressed in Arabidopsis *uvr8* null mutant plants. The presence of

Chlamydomonas orthologs for additional known UV-B signaling players, including Cr-COP1 shown to partake in a typical Cr-UVR8/Cr-COP1 UV-B photocycle, a putative At-HY5 ortholog (Cre06.g310500), and a putative At-RUP1/At-RUP2 ortholog (Cre01.g053850), further indicates evolutionary conservation of the canonical UVR8 UV-B signaling pathway.

COP1 proteins also show functional conservation between diverse phototrophic eukaryotes, as demonstrated recently between *Physcomitrella patens*, rice (*Oryza sativa*), and Arabidopsis (Ranjan et al., 2014), suggesting widespread presence of the UVR8/COP1 UV-B photocycle. However, in addition to the conserved activity of COP1 in UV-B signaling, it is presently unclear whether in Chlamydomonas Cr-COP1 acts as a repressor of physiological responses analogous to photomorphogenesis in flowering plants and whether Chlamydomonas cryptochrome photoreceptors signal through Cr-COP1. A comprehensive characterization of the role Cr-COP1 plays in Chlamydomonas aside from UV-B signaling may shed light on how COP1 function evolved in higher plants, leading to a more comprehensive understanding of this multifaceted protein. Of note, humans have a version of COP1 (Yi and Deng, 2005), indicating its far-reaching

Table 1. UV-B-Responsive Genes in Chlamydomonas and Their Functional Classification

Gene Identifier	LogFC	Annotation (Phytozome 10.2)
Cre01.g016600	10.17	Photosynthesis. PSII-associated 22-kD protein; *PSBS1*
Cre01.g016750	8.68	Photosynthesis. PSII 22-kD protein; *PSBS2*
Cre07.g320400	5.34	Photosynthesis. Chlorophyll *a/b* binding protein
Cre01.g021800	4.87	SET domain-containing protein, histone-lysine *N*-methyltransferase-related
Cre07.g320450	4.79	Photosynthesis. Chlorophyll *a/b* binding protein.
Cre08.g367500	4.78	Photosynthesis. Chlorophyll *a/b* binding protein, stress-related chlorophyll *a/b* binding protein 2; *LHCSR3.1* (alias *LHCSR2*)
Cre04.g211850	4.58	Photosynthesis. Chlorophyll *a/b* binding protein; *ELI5*
Cre06.g278267	4.18	No annotation available
Cre14.g626750	4.09	Photosynthesis. Chlorophyll *a/b* binding protein, EARLY LIGHT-INDUCED PROTEIN1, CHLOROPLASTIC-RELATED
Cre10.g460326	4.01	No annotation available
Cre08.g367400	3.95	Photosynthesis. Chlorophyll *a/b* binding protein, stress-related chlorophyll *a/b* binding protein 3; *LHCSR3.2* (alias *LHCSR3*)
Cre07.g344500	3.90	Glycosyl transferase family 90, protein xylosyltransferase-related, KDEL (LYS-ASP-GLU-LEU) CONTAINING - RELATED
Cre02.g143450	3.88	Protein of unknown function (DUF4079)
Cre17.g740950	3.70	Photosynthesis. Chlorophyll *a/b* binding protein, high-intensity light-inducible LHC-like gene; *LHL4* (alias *ELI6*)
Cre08.g376250	3.70	Sphingomyelin phosphodiesterase related
Cre16.g677800	3.62	TraB family protein
Cre03.g159581	3.56	mTERF (PFAM)
Cre04.g222750	3.56	Mitochondrial carrier protein, low-CO_2-inducible chloroplast envelope protein; *CCP2*
Cre17.g719500	3.53	Flavin-containing amine oxidoreductase, phytoene desaturase; *AOF9*
Cre12.g521650	3.50	Thioesterase domain, diacylglycerol acyltransferase
Cre06.g280150	3.49	Photosynthesis. PsbP-like protein; *PSBP9*
Cre12.g492650	3.43	Fasciclin-like protein; *FAS2*
Cre11.g467672	3.36	Cys-rich secretory protein family, defense-related protein-containing SCP domain
Cre04.g215050	3.35	Fatty acid hydroxylase superfamily, β-carotene hydroxylase, putative chloroplast precursor; *CBH1* (alias *CHYB*, *CHYB1*)

Listed are genes that show >10-fold upregulation following 1 h of UV-B exposure. The complete RNA-seq data set is in Supplemental Data Set 1. LogFC, $\log_2$ fold change.

evolutionary conservation, although there is no evidence for a human UVR8 counterpart for UV-B perception.

Taken together, our results suggest wide conservation of the UVR8 photoreceptor and UV-B signaling pathway over a remarkable evolutionary distance. Moreover, conservation of the number and position of key residues, including Trps and salt-bridging Args, strongly suggests that all UVR8 photoreceptor proteins function with a similar molecular mechanism. It is clear that a UVR8-mediated UV-B perception and signaling pathway must have existed in a shared common ancestor of Chlamydomonas and Arabidopsis >1000 million years ago, perhaps helping photosynthetic organisms to colonize environments with high levels of incidental UV-B (Rozema et al., 1997; Gutman and Niyogi, 2004).

UV-B Acclimation and Tolerance in Chlamydomonas

A clear UV-B acclimation effect was seen in Chlamydomonas colony survival following UV-B stress and in Chlamydomonas cultures when using the chlorophyll fluorescence parameter Fv/Fm as a measure of UV-B-induced photoinhibition. UV-B stress exposure resulted in UV-B-induced photoinhibition that was ameliorated by prior UV-B acclimation. When chloroplast translation was blocked using CAM, greater UV-B-induced photoinhibition was observed in response to UV-B stress, and, interestingly, both UV-B-acclimated and nonacclimated cultures were affected to the same extent. The UV-B-induced photoinhibition we observed following broadband UV-B stress is presumably due to UV-B-induced PSII damage that exceeds the rate of repair (Takahashi et al., 2010; Takahashi and Badger, 2011). PSII subunit D1 in particular is a well known photosynthetic target of UV-B damage (Jansen et al., 1996; Takahashi et al., 2010), and photoinhibition has long been associated with a decrease in D1 and, albeit to a lesser extent, D2 protein level (Schuster et al., 1988). In agreement, we observed decreases in D1 and D2 protein levels in UV-B-exposed Chlamydomonas that correlated well with the extent of UV-B-induced photoinhibition. Our observed D1 and D2 protein decrease accompanied by photoinhibition following UV-B stress agrees with previous studies (Schuster et al., 1988; Booij-James et al., 2000; Chaturvedi and Shyam, 2000; Wu et al., 2011). When chloroplast translation was blocked, D1 and D2 protein levels were also lower in response to UV-B stress and decreased to the same extent in both UV-B-acclimated and nonacclimated cultures. This implies that at least part of the UV-B acclimation effect on maintaining photosynthetic efficiency involves a faster rate of de novo D1 and D2 synthesis within chloroplasts, similar to the processes observed with high-light acclimation in pea (*Pisum sativum*; Aro et al., 1993) and recovery following UV-B inactivation of photosynthesis in Chlamydomonas (Chaturvedi and Shyam, 2000).

A more direct role for UVR8 UV-B signaling in Chlamydomonas UV-B acclimation could be established by performing similar experiments to those we present here alongside a mutant strain where the function of Cr-UVR8 is impaired. However, such a mutant strain remains to be generated, despite our best efforts to knock out/down Cr-*UVR8* using codon optimized TALEN as well as artificial microRNA approaches (Molnar et al., 2009; Boch, 2011). Of note, an artificial microRNA developed
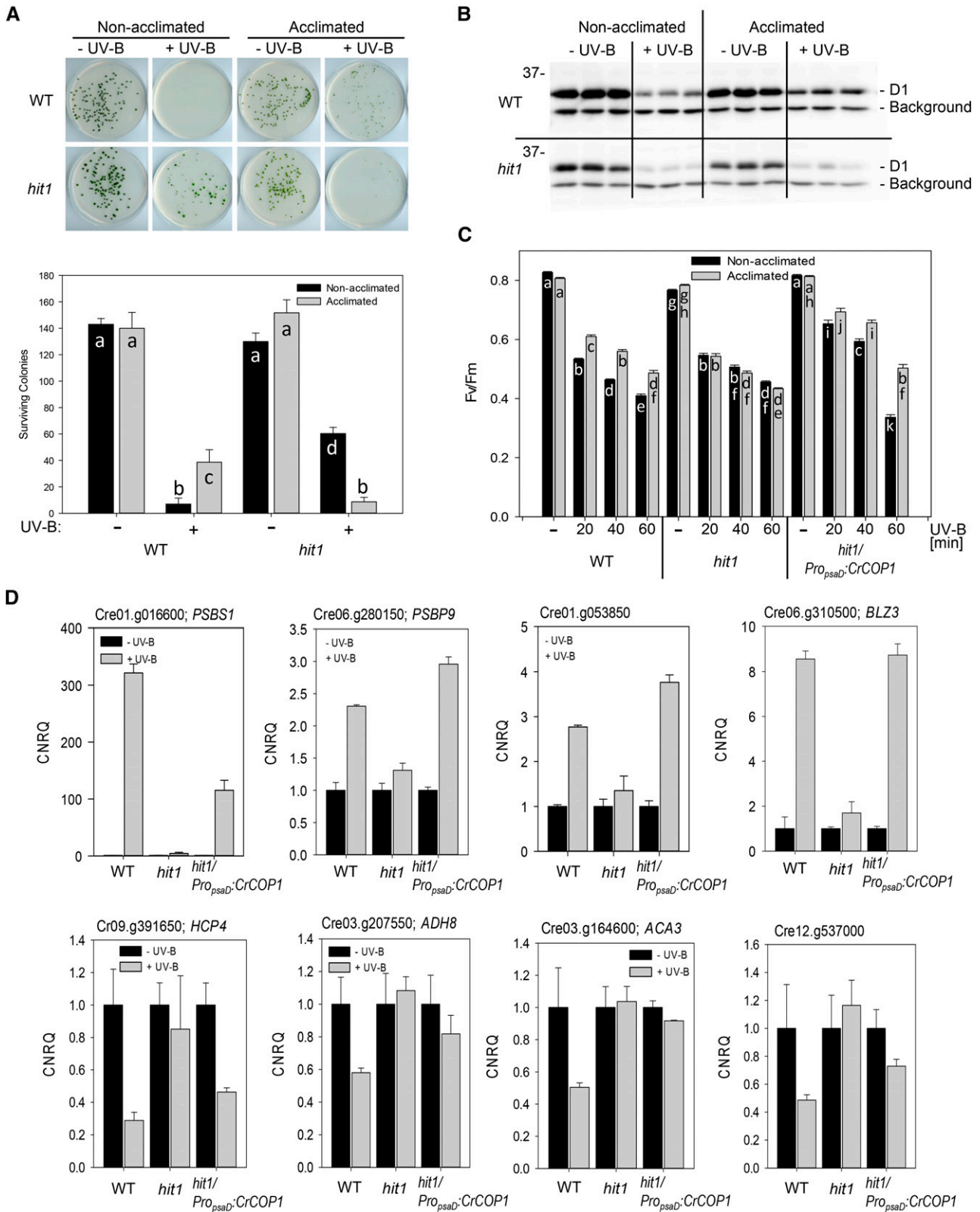
Figure 7. Cr-COP1 Activity Is Required for UV-B Acclimation in Chlamydomonas.

concurrently to target Arabidopsis UVR8 was successfully used to generate lines where UVR8 was physically and functionally absent (Vandenbussche et al., 2014). Nevertheless, a mutant Chlamydomonas strain was recently identified that displayed enhanced high-light tolerance and was found to have an amino acid substitution in the WD40 domain of Cr-COP1 (reported as LRS1) (Schierenbeck et al., 2015). Since in Arabidopsis the interaction of COP1 with UVR8 is at the base of the UV-B signaling pathway, the *hit1* strain was used in our experiments to investigate the dependence of UV-B acclimation on Cr-UVR8 signaling. By analyzing Chlamydomonas colony survival, maintenance of D1 protein and a prevention of UV-B-induced photoinhibition following UV-B stress, UV-B acclimation was clearly found to be abolished in the *hit1* strain. However, it should be noted that a greater basal resistance to UV-B stress was observed in non-UV-B-acclimated *hit1* colonies. Such a phenomenon may be the result of a constitutive *hit1* phenotype in the absence of UV-B due to its potential role as repressor of light responses similar to Arabidopsis *cop1* mutant plants (Yi and Deng, 2005; Schierenbeck et al., 2015). Further experiments based on UV-B-induced photoinhibition alone showed that UV-B acclimation was subsequently restored in *hit1/Pro_{psaD}:CrCOP1* complementation strains, indicating that UV-B acclimation phenotypes are dependent on a Cr-UVR8-CrCOP1 interaction under UV-B.

The potential role of UVR8 UV-B signaling in photosynthesis is a current and interesting question. Recent work has begun to address this and has shown in Arabidopsis that UVR8 plays a role in maintaining photosynthetic efficiency under elevated UV-B (Davey et al., 2012). D1 protein levels were also investigated; however, the authors did not observe any difference in the magnitude of D1 protein decrease under UV-B between wild-type and *uvr8* plants. While this study does highlight an interesting involvement of UVR8, it does not address the role of UV-B acclimation in maintaining photosynthetic efficiency under elevated UV-B. It is of interest whether UV-B-acclimated plants would maintain photosynthetic efficiency and whether this process was abolished in *uvr8* plants. Similarly, levels of the D1 protein might be preserved under elevated UV-B in UV-B-acclimated plants and this may depend on UVR8. However, the question remains what the linking mechanisms would be between UVR8 UV-B signaling

and D1/D2 protein resynthesis in the chloroplast. Involvement of nuclear regulators of chloroplastic *psbA* (encoding D1) and *psbD* (encoding D2) expression and mRNA stability would be likely. Interestingly, the Chlamydomonas nuclear *NAC2* is among the UV-B-induced genes in our transcriptomic analysis (2.5-fold), and its product, the chloroplast TPR-like NAC2 protein, is important for *psbD* mRNA stability (Boudreau et al., 2000). Also, it is possible that UV-B-induced secondary metabolites interact with thylakoid membranes and promote efficient damage repair (Dobrikova and Apostolova, 2015; Järvi et al., 2015). However, these and several other mechanisms can be envisaged and need to await experimental verification.

Independent of D1 and D2, it should be noted that our RNA-seq analysis (see also below) has identified a large number of genes that are associated with photosynthesis and play a predicted role in photoprotection are regulated by UV-B (including *PSBS1*, *PSBS2*, *LHCSR1*, *LHCSR3.1*, and *LHCSR3.2*), all of which may be implicated in retaining photosynthetic efficiency through UV-B acclimation. The PSBS proteins play an essential role in energy-dependent nonphotochemical quenching (NPQ) in land plants, a mechanism that rapidly promotes heat dissipation of excess light energy collected by the light-harvesting antenna (Niyogi and Truong, 2013). In Chlamydomonas, however, the PSBS protein has so far not been detected nor shown to play a role in NPQ (Bonente et al., 2008). The high light-induced LHCSR proteins are essential for NPQ in Chlamydomonas and other green algae but are absent in vascular plants (Peers et al., 2009). Thus, the question arises whether in Chlamydomonas UV-B is perceived as a proxy for high-light exposure to trigger acclimation responses and photoprotection. Alternatively, the process of UV-B acclimation may alleviate the consequences of damage inflicted by UV-B to the oxygen-evolving complex. The latter normally provides electrons to rapidly rereduce PSII that has been oxidized by light-driven charge separation. When the oxygen-evolving complex is damaged, downregulation of light harvesting in response to UV-B could limit the formation of oxidized PSII and ensuing damage caused by this powerful oxidant.

When considering the interplay between UV-B and photosynthesis, there is a general view that UV-B exerts an overall deleterious effect, and photosynthetic yield would be greatly enhanced in its absence. However, the way UV-B experiments are

---

Figure 7. (continued).

(A) Survival of Chlamydomonas UV-B-acclimated and nonacclimated colonies following broadband UV-B stress. Top: Representative plates used to quantitate surviving colonies, scanned following 4 d (−UV-B stress treatment) or 8 d growth (+UV-B stress). Bottom: Quantification of surviving colonies. −UV-B, no broadband UV-B stress; +UV-B, 4 h broadband UV-B stress exposure. Means and SE are shown (*n* = 3). Shared letters indicate no statistically significant difference in the means (P > 0.05).

(B) Immunoblot analysis of D1 protein level in triplicate cultures of UV-B-acclimated or nonacclimated Chlamydomonas strains before (−UV-B) and following (+UV-B) broadband UV-B stress.

(C) UV-B-induced photoinhibition in Chlamydomonas strains as measured by a decrease of the maximum quantum yield of PSII (Fv/Fm) following broadband UV-B stress. Means and SE are shown (*n* = 3). Nonacclimated, grown under weak white light only; Acclimated, grown under equivalent white light supplemented with narrowband UV-B; −UV-B, no broadband UV-B stress; 20/40/60 UV-B, duration of broadband UV-B stress exposure (min). Shared letters indicate no statistically significant difference in the means (P > 0.05).

(D) Cr-COP1 activity is required for UV-B-induced expression changes of select Chlamydomonas genes. Individual RT-qPCR analysis of select Chlamydomonas genes. Expression of each gene following 1 h UV-B (+UV-B) is normalized to levels in −UV-B control samples (−UV-B). WT, CC-124 (137c mt-); *hit1*, Cr-*COP1* mutant; *hit1/Pro_{psaD}:CrCOP1*, *hit1* complemented by Cr-*COP1* expression driven by the *psaD* promoter. CNRQ, calibrated normalized relative quantities.

performed in controlled environments can create artificial situations that would rarely occur in nature whereby photosynthetic organisms are subject to higher than ambient levels of UV-B without any prior exposure. It has recently been suggested that UV-B exposure in a manner allowing UV-B acclimation leads to higher photosynthetic rates and cross-photoprotection resulting in higher final photosynthetic yield (Wargent et al., 2011, 2015). With the current use of glasshouses and UV-B-impermeable cladding in modern agriculture, the precise relationship between UV-B and photosynthesis is important to define in detail.

Global Transcriptomic Analysis of UV-B Acclimation in Chlamydomonas

Continuous low-level narrowband UV-B exposure allows UVR8-mediated UV-B acclimation in Arabidopsis, experimentally shown as increased UV-B tolerance during a subsequent UV-B stress treatment in the wild type, but not in *uvr8* mutants (Favory et al., 2009; Gruber et al., 2010; González Besteiro et al., 2011). Under these conditions, Arabidopsis seedlings can grow and acclimate for many days without displaying UV-B stress symptoms. Using the same low-level narrowband UV-B exposure, a previous genome-wide microarray experiment of Arabidopsis wild type in comparison to *uvr8* and *cop1* mutants showed that >97% of genes induced after both 1 and 6 h of UV-B are UVR8 and COP1 dependent (Favory et al., 2009). It should be noted that the UVR8-dependent transcriptome response in Arabidopsis involves induction of a number of stress-related genes, for example, the *EARLY LIGHT-INDUCED PROTEIN1* (*ELIP1*) and *ELIP2* encoding stress-related chlorophyll *a/b* binding family proteins, and *UV RESISTANCE2/PHOTOREACTIVATING ENZYME1* (*UVR2/PHR1*), encoding a photolyase DNA repair enzyme (Favory et al., 2009). However, the clear role for UVR8 in this process demonstrates that activity of the UV-B photoreceptor, rather than a general UV-B stress, is causal for induction of these stress-related genes.

In this study, we designed UV-B treatment conditions using a similar approach in order to analyze Chlamydomonas transcriptome changes during a likely UV-B acclimation response. The same low-level narrowband UV-B shown to induce UV-B acclimation was applied, and global gene expression changes following 1 h of exposure were analyzed by RNA-seq. Similar to the UVR8-mediated UV-B transcriptome in Arabidopsis, many of the induced genes can be associated with UV-B stress protection and/or damage repair. Such gene associations were expected from the UV-B acclimation observed in cultures grown under the same exposure levels. The similarities between our designed RNA-seq growth conditions and those demonstrated specifically to deploy a UVR8-dependent UV-B transcriptome in Arabidopsis imply that our RNA-seq data are also a reflection of a Chlamydomonas UV-B response governed by its Cr-UVR8 UV-B photoreceptor. Even though at present we cannot unequivocally link all identified UV-B-responsive genes directly to Cr-UVR8 and Cr-COP1, they underlie the physiological response of Chlamydomonas to low-level acclimatory UV-B.

Similar to the lack of UVR8-associated gene expression changes following UV-B exposure of Arabidopsis *cop1* plants (Oravecz et al., 2006), the *hit1* strain was impaired in UV-B-responsive expression changes of several UV-B marker genes. For most of these genes, this phenotype could be complemented by expression of the wild-type Cr-*COP1* gene. This highlights that Cr-COP1 is required at least for some of the UV-B-responsive expression changes in Chlamydomonas, likely via a UV-B-dependent interaction with Cr-UVR8. We thus conclude that the transcriptome changes described here will provide an important basis for a further detailed understanding of UVR8 signaling and UV-B acclimation in Chlamydomonas.

In summary, here we describe evolutionarily conserved UVR8 UV-B perception and signaling in Chlamydomonas. This underlines the evolutionary conservation of UVR8 UV-B signaling and its importance for life under sun exposure. Also, this work establishes Chlamydomonas as a novel model platform to study UV-B signaling. In addition, we demonstrate that Chlamydomonas UV-B acclimation can prevent UV-B-induced photoinhibition and that this process modifies rates of D1 and D2 protein repair. Future work can combine these two research themes using Chlamydomonas as a model system to dissect the relationship between UVR8 UV-B signaling, UV-B exposure, and photosynthesis.

METHODS

Plant Material, Growth Conditions, and UV-B Irradiation

Arabidopsis thaliana plants used in this work were of wild-type accession Col-0 and the T-DNA insertion line *uvr8-6* (Favory et al., 2009). Arabidopsis was transformed with binary vectors described below by the floral dip method (Clough and Bent, 1998). The transgenic Arabidopsis lines generated in this work were shown through segregation analysis to have the transgene integrated at a single genetic locus. Plants for analysis were taken from the homozygous T3 generation. Experimental Arabidopsis seedlings were grown from surface-sterilized seeds on plates using half-strength Murashige and Skoog plates containing 1% sucrose and 1% phytagel (Sigma-Aldrich).

Chlamydomonas reinhardtii CC-125 wild-type strain (137c mt+) was used in this work, except in experiments using the *hit1* mutant, which is in the CC-124 (137c mt-) background (Schierenbeck et al., 2015). Chlamydomonas was grown using Tris acetate phosphate (TAP) media (Gorman and Levine, 1965) with mineral nutrient supplements (Kropat et al., 2011). A working stock of Chlamydomonas was maintained on solid TAP media containing 1.6% Bacto agar (Difco) and was subcultured biweekly. Experimental Chlamydomonas cells were cultured in liquid TAP media.

For UV-B experiments, Arabidopsis seedlings and Chlamydomonas cultures were grown under constant weak light (3.6 µmol m^{-2} s^{-1}) with supplemental narrowband UV-B (0.07 mW/cm^2, measured with a VLX-3W UV light meter equipped with a CX-312 sensor; Vilber Lourmat) using Osram L18W/30 white-light and Philips TL20W/01RS narrowband UV-B tubes, as previously described (Oravecz et al., 2006; Favory et al., 2009). UV-B was either applied or blocked using filters of the WG series (Schott Glaswerke) with half-maximal transmission at 311 and 360 nm, respectively (Ulm et al., 2004). For Cr-UVR8 monomerization, cells from cultures at stationary growth stage were exposed to 30 min broadband UV-B (2 mW/cm^2, VLX-3W/CX-312 UV light meter) and then allowed to recover in white light devoid of UV-B. Cell samples were collected immediately after UV-B treatment and after 2 and 4 h of white light recovery.

Cloning of Cr-*UVR8* and Cr-*COP1*

Total RNA was extracted from Chlamydomonas cells using an RNeasy Mini kit (Qiagen) following the manufacturer's instructions. Purified RNA was

treated using an RNase-Free DNase Set (Qiagen). DNase was heat in-activated in the presence of 2 mM EDTA and then RNA was subject to a cleanup protocol using an RNeasy Mini kit (Qiagen). cDNA synthesis was performed using Taqman Reverse Transcription Reagents (Applied Bio-systems). Cr-*UVR8* (Cre05.g230600) was PCR amplified with attB rec-ognition sequences for Gateway cloning using the primers CrUVR8attB1 Fd and CrUVR8attB2 Rv (see Supplemental Table 1 for primer sequences). A version of Cr-*UVR8* without a stop codon for fusion of CFP to the C terminus was PCR amplified using the primers CrUVR8attB1 Fd and CrUVR8(-stop)attB2 Rv (Supplemental Table 1). Cr-*UVR8* and Cr-*UVR8 (-stop)* amplified sequences were cloned into pDONR207 and sequenced to check integrity of the cloned fragment. Cr-*UVR8* was then inserted into the binary destination vectors pB2GW7 for 35S-driven expression in plants, pB7WGC2 for plant expression with N-terminal fusion of CFP (Karimi et al., 2002), and Gateway-compatible yeast two-hybrid vectors described below. Cr-*UVR8(-stop)* was inserted into pB7CWG2 for plant expression with C-terminal fusion of CFP (Karimi et al., 2002). Cr-*COP1* (Cre02.g085050) was PCR amplified from cDNA using primers CrCOP1 Fd and CrCOP1 Rv (Supplemental Table 1) and cloned into vector pCR2.1-TOPO (Life Technologies). From this clone, Cr-*COP1* was PCR amplified again with attB recognition sequences for Gateway cloning using the primers CrCOP1attB1 Fd and CrCOP1attB2 Rv (Supplemental Table 1), cloned into pDONR207, and sequenced to check integrity of the cloned fragment. Cr-*COP1* was then inserted into Gateway-compatible yeast two-hybrid vectors described below.

Chlamydomonas Transformation

The Cr-*COP1* coding sequence was cloned between the *psaD* promoter and terminator in a Gateway-compatible derivative of pSL18, which contains an *aphVII* gene cassette conferring paromomycin resistance (Depège et al., 2003). *hit1* mutants were transformed with pSL18-GW-CrCOP1 by electroporation (Shimogawara et al., 1998; Kuras et al., 2007) and transformants were selected by growth on paromomycin.

Chlamydomonas UV-B Acclimation Assay and Chloroplast Translation Inhibition

Chlamydomonas cultures were grown in deep Petri dishes fixed to a large orbital shaker (Infors HT). Sufficient culture volume of 0.5×10^6 cells/mL was obtained by diluting a 2-d-old 10-mL starter culture grown in an Erlenmeyer flask. Fifteen milliliters of 0.5×10^6 cells/mL culture was placed in each sterile Petri dish and filters described above were used as lids, secured by pressing them onto a small lip of Parafilm stretched over the upper rim of each dish. Each Chlamydomonas plate culture was placed in a UV-B-supplemented weak-light field where it was exposed to 3.6 µmol m^{-2} s^{-1} PAR (measured with a LI-250 light meter; LI-COR Biosciences) and, if intended, 0.07 mW/cm^2 narrowband UV-B (un-derneath a 311-nm filter). Plate cultures were shaken at 90 rpm. For growth rate experiments, replicate plate cultures were sampled periodically and cell density was quantified using a hemocytometer. For UV-B acclimation experiments, plate cultures were grown for 4 d before cells were sampled. Two-milliliter volumes of 4-d-old plate cultures were placed into 60-mm-diameter Petri dishes covered by filters described above then subject to broadband UV-B stress treatment (Philips TL40W/12RS; 2 mW/cm^2, VLX-3W/CX-312 UV light meter) for varying times. Treated cultures were then either collected by centrifugation and pellets frozen for downstream molecular analysis or used directly for chlorophyll fluorescence mea-surements to assay the maximum quantum yield of PSII (Fv/Fm). Samples were moved into glass vials compatible with the chamber of a plant effi-ciency analyzer (PEA MK2; Hansatech Instruments), dark-adapted for 5 min, and then Fv/Fm was measured. For those experiments where chloroplast translation was blocked, 4-d-old Chlamydomonas plate

cultures were supplemented with CAM (dissolved in water; Sigma-Aldrich) to a final concentration of 100 µg/mL. Chemical inhibition was allowed to proceed for 30 min before commencing broadband UV-B stress treatment. Average Fv/Fm values were compared by one-way ANOVA (Holm-Sidak method) using SigmaPlot version 12.5.

Chlamydomonas Colony Survival UV-B Acclimation Assay

Chlamydomonas cells were adapted to low-light conditions by growing a 3-d-old plate culture as described above. Cultures were diluted to 100 cells per 100 µL, which were plated onto solid media and allowed to grow for 4 d exposed to 3.6 µmol m^{-2} s^{-1} PAR and, if intended, 0.07 mW/cm^2 narrowband UV-B (underneath a 311-nm filter). Established colonies were then treated for 4 h with broadband UV-B, as described above. Treated plates were kept in low light and surviving colonies were counted after 10 d further growth. Average colony numbers were compared by one-way ANOVA (Holm-Sidak method) using SigmaPlot version 12.5.

Arabidopsis Hypocotyl Measurements

Seed for assayed lines were sown evenly spaced on duplicate plates and stratified at 4°C for 48 h in darkness before being moved to either –UV-B (3.6 µmol m^{-2} s^{-1} PAR) or +UV-B (equivalent PAR with 0.07 mW/cm^2 supplemental UV-B underneath a 311-nm filter) conditions. Seedlings were grown for 4 d before being transplanted and placed horizontally on 1% agar plates. Seedling plates were scanned and hypocotyl lengths were measured using ImageJ.

Yeast Two-Hybrid Assays

Protein interaction was assayed using the LexA yeast two-hybrid system with Cr-*UVR8* cloned into Gateway-compatible vector pBTM116-D9-GW in frame with the LexA DNA binding domain (BD) and both AtCOP1 and CrCOP1 cloned into vector pGADT7-GW in frame with the Gal4 activation domain (AD). BD and AD vectors were cotransformed into yeast strain L40 and the resulting colonies surviving on -Trp/-Leu medium were used for chlorophenol red-β-D-galactopyranoside (Roche Applied Science) quan-titative protein interaction assays, as previously described (Rizzini et al., 2011). If needed, yeast cells were irradiated by narrowband UV-B (Philips TL20W/01RS; 20 h, 1.5 µmol m^{-2} s^{-1}) (Rizzini et al., 2011; Yin et al., 2015).

Protein Extraction and Immunoblot Analysis

Rabbit polyclonal antibodies were raised and affinity purified against the peptide WGRGEDGQLGHGQADQ (Cr-UVR8[34-49]; Eurogentec). For UVR8 dimer/monomer visualization, total Chlamydomonas protein was ex-tracted in 50 mM Tris, pH 7.6, 150 mM NaCl, 2 mM EDTA, 1% Igepal (Sigma-Aldrich), 1% (v/v) protease inhibitor cocktail for plant extracts (Sigma-Aldrich), 10 µM MG132, and 10 µM ALLN. For analysis of Arabidopsis lines, total protein was extracted in the same buffer with the addition of 10% glycerol and 5 mM MgCl$_2$. For D1 and D2 protein detection, total Chlamydomonas protein was extracted in 50 mM Tris, pH 7.6, 2% (v/v) SDS, and 2% (v/v) protease inhibitor cocktail for plant extracts (Sigma-Aldrich). For protein gel blot analysis, total cellular proteins were separated by electrophoresis in SDS-PAGE gels and transferred to PVDF membranes according to the manufacturer's instructions (Bio-Rad). In the gels where detection of Cr-UVR8 was desired, gels were exposed to 10 min of broadband UV-B (2 mW/cm^2) prior to transfer, as established for the analysis of At-UVR8 before (Rizzini et al., 2011). Primary antibodies used were polyclonal anti-CrUVR8[34-49] (this work), anti-AtUVR8[426-440] (Favory et al., 2009), anti-CHS (sc-12620; Santa Cruz Biotechnology), anti-actin (A0480; Sigma-Aldrich), and anti-D1 and anti-D2 (a gift from Jean-David Rochaix, University of Geneva, Switzerland). Secondary antibodies were

anti-rabbit or anti-goat immunoglobulins (DAKO), as appropriate. Chemiluminescent signals were generated using the ECL Western Detection Kit and detected with an ImageQuant LAS 4000 mini CCD camera system (GE Healthcare). For D1 and D2 protein analysis, levels were quantified using ImageQuant TL software (GE Healthcare) with manual annotation of lane cutoffs on each blot. Three biological replicates were used to calculate average band volume for each treatment, which was then normalized to average band volume in control samples. Normalized average band volumes were compared by one-way ANOVA (Holm-Sidak method) using SigmaPlot version 12.5.

RNA-Seq and Transcriptome Analysis

For expression analysis in Chlamydomonas in response to UV-B, six 15-mL plate cultures were grown under weak light for 4 d before three cultures were exposed to 1 h of narrowband UV-B (0.07 mW/cm^2). Two milliliters of each culture was sampled following UV-B treatment and pellets of cells were frozen immediately. Total RNA was extracted with a NucleoSpin RNA II Total RNA isolation kit (Machery-Nagel), and final RNA samples were DNase treated. Stranded RNA-seq analysis of the above six RNA samples (three −UV-B, three 1 h +UV-B) was performed in conjunction with the iGE3 genomics platform of the University of Geneva (http://www.ige3.unige.ch/genomics-platform.php). The libraries were prepared with 400 ng of total RNA as starting material and processed with the Illumina TruSeq RNA stranded kit according to the manufacturer's instructions. The Accuprime High Fidelity PCR enzyme was used in the DNA fragment enrichment step. Sequencing quality control was done with FastQC (http://www.bioinformatics.babraham.ac.uk/projects/fastqc/). The length of reads was 100 single reads. The reads were mapped using TopHat v.2 (Trapnell et al., 2009) to the *Chlamydomonas reinhardtii* 236 release reference (Phytozome v10.2) on new junctions and known junctions annotations. Counts of the number of reads mapping to each gene feature of *Chlamydomonas reinhardtii* 236 reference were prepared with HTSeq v0.5.3p9 (htseq-count; http://www-huber.embl.de/users/anders/HTSeq/). Differential expression analysis was performed with the statistical analysis R/Bioconductor package EdgeR v. 3.4.2 (Robinson et al., 2010). Briefly, the counts were normalized according to the library size and filtered. Those genes having a count above 1 count per million reads in triplicate samples were kept for the analysis. The differentially expressed genes tests were performed using exact negative binomial test statistics. Differentially expressed genes with >2-fold change between conditions and FDR < 0.05 were plotted in R using the heatmap.2 function.

RNA-seq data have been deposited in NCBI's Gene Expression Omnibus (Edgar et al., 2002) and are accessible through GEO Series accession number GSE68739. Coverage of RNA-seq data is shown in Supplemental Table 2.

For transcriptome comparison, genes with significantly altered expression (FDR ≤ 0.05 and FC ≥ 2 or FC ≤ −2) resulting from UV-B treatment were compared with those genes with significant differential regulation following a dark-to-light transition, as previously described (Duanmu et al., 2013). Genes that were updated in Phytozome 10 compared with Phytozome 9 have been updated using the Phytozome 10 transfer tables as far as possible. A hypergeometric test was applied to evaluate the significance of shared genes between the two data sets. In order to normalize the data sets prior plotting, a z-score was calculated for both over all expressed genes and differently expressed genes were plotted against each other.

Quantitative RT-PCR

For UV-B expression induction of *HY5* and *CHS* in Arabidopsis, seedlings were grown for 4 d on plates in constant weak light before narrowband UV-B was applied for the times indicated. An RNeasy Plant Mini Kit (Qiagen) was used to extract total RNA. Contaminating DNA in final RNA samples was removed using an RNase-Free DNase set (Qiagen). DNase was heat inactivated in the presence of 2 mM EDTA and treated RNA samples were used directly. cDNA synthesis was performed using Taqman Reverse Transcription Reagents (Applied Biosystems). Relative transcript abundance of target genes was determined using ABsolute QPCR SYBR Green ROX Mix, an ABI 7900 HT Fast Real-Time PCR system in conjunction with Sequence Detection Systems software version 2.4 (Applied Biosystems), and qbasePLUS real-time PCR data analysis software version 2.4 (Biogazelle). A normalization factor was generated based on transcript levels of UV-B-stable Arabidopsis *18S* rRNA and *UBIQUITIN-PROTEIN LIGASE7* (*UPL7*, At3G53090), which was used to normalize expression levels of *HY5* and *CHS*. Primer sequences are detailed in Supplemental Table 1. Melt curve analysis was performed for each individual RT-qPCR reaction to ensure a single product was amplified.

To confirm the RNA-seq data, Chlamydomonas was treated as were samples used for RNA-seq, and cDNA synthesis and RT-qPCR were performed as above. A normalization factor was generated based on transcript levels of Chlamydomonas reference genes *Cre06.g6364* (*RACK1*) and *Cre03.g159200* (At-*UPL7* ortholog), tested prior for expression stability under UV-B experimental conditions, which was used to normalize expression levels of *Cre01.g016600* (*PSBS1*), *Cre06.g280150* (*PSBP9*), *Cre01.g053850* (WD40 repeat-containing protein; AtRUP1/RUP2-like), *Cre06.g310500* (bZIP transcription factor, *BLZ3*; AtHY5-like), *Cre06.g278251* (*aCRY*), *Cre12.g537000*, *Cre03.g164600* (*ACA3/PMA3/PMH1*), *Cre03.g207550* (*ADH8*), and *Cre09.g391650* (*HCP4*). Primer sequences are detailed in Supplemental Table 1.

Protein Structure Modeling

The full-length Cr-UVR8 amino acid sequence was submitted to the Web-based structure predicted servers I-TASSER (Zhang, 2008), SWISS-MODEL (Arnold et al., 2006), and RaptorX (Peng and Xu, 2011) using At-UVR8 as a template (PDB ID 4D9SA). All of the returned models showed similar three-dimensional Cr-UVR8 structures. The model generated by Raptor X carried the lowest P value (1.49e-23) and was selected as the most reliable. The PyMOL Molecular Graphics System Version 1.5.0.4 (Schrödinger) was used to visualize and refine the depicted three-dimensional At-UVR8 (PDB ID 4D9SA) and Cr-UVR8 (RaptorX model) structures.

Accession Numbers

RNA-seq data reported in this article have been deposited in NCBI's Gene Expression Omnibus (Edgar et al., 2002) and are accessible through GEO Series accession number GSE68739. Arabidopsis sequence data from this work can be found in The Arabidopsis Information Resource (https://www.arabidopsis.org/) database under the following accession numbers: AT5G13930 (*CHS*), AT2G32950 (*COP1*), AT5G11260 (*HY5*), and AT5G63860 (*UVR8*). Chlamydomonas sequence data can be found in Phytozome (http://phytozome.jgi.doe.gov/): Cre06.g310500, Cre01.g053850, Cre02.g085050 (*COP1/LRS1*), and Cre05.g230600 (*UVR8*). The experimentally determined Cr-*UVR8* and Cr-*COP1* coding sequences reported here are available in GenBank (accession numbers KP780811 and KP780812, respectively).

Supplemental Data

Supplemental Figure 1. Protein alignment of At-UVR8 with Cr-UVR8.

Supplemental Figure 2. Transgenic expression of *CrUVR8-CFP* and *CFP-CrUVR8* in Arabidopsis complements the *uvr8* mutant UV-B phenotype.

Supplemental Figure 3. Low-level UV-B delays Chlamydomonas culture growth.

Supplemental Figure 4. Chloramphenicol usage to block chloroplast translation.

Supplemental Figure 5. Comparison of differentially expressed genes in response to supplemental UV-B and white light during dark-to-light transition.

Supplemental Table 1. Primer sequences used in this study.

Supplemental Table 2. Coverage of RNA-seq data.

Supplemental Data Set 1. UV-B-responsive genes in Chlamydomonas.

Supplemental Data Set 2. Comparison of UV-B treatment and dark-to-light transition: induced genes.

Supplemental Data Set 3. Comparison of UV-B treatment and dark-to-light transition: repressed genes.

AUTHOR CONTRIBUTIONS

K.T. and R.U. conceived and designed the research. M.G.-C. contributed to the experimental design. K.T. performed all experiments, except the colony survival UV-B acclimation assay that was performed by M.D., the yeast two-hybrid experiments that were performed by R.Y., and *hit1* mutant and complementation analysis that was performed by R.C. and G.A. C.D.C. performed protein structure modeling and E.S.-S. performed the comparative RNA-seq analysis. K.T., M.G.-C., and R.U. analyzed the data. K.T. and R.U. wrote the article. All authors read, revised, and approved the article.

REFERENCES

Arnold, K., Bordoli, L., Kopp, J., and Schwede, T. (2006). The SWISS-MODEL workspace: a web-based environment for protein structure homology modelling. Bioinformatics **22:** 195–201.

Aro, E.M., McCaffery, S., and Anderson, J.M. (1993). Photoinhibition and D1 protein degradation in peas acclimated to different growth irradiances. Plant Physiol. **103:** 835–843.

Beel, B., Prager, K., Spexard, M., Sasso, S., Weiss, D., Müller, N., Heinnickel, M., Dewez, D., Ikoma, D., Grossman, A.R., Kottke, T., and Mittag, M. (2012). A flavin binding cryptochrome photoreceptor responds to both blue and red light in *Chlamydomonas reinhardtii*. Plant Cell **24:** 2992–3008.

Binkert, M., Kozma-Bognár, L., Terecskei, K., De Veylder, L., Nagy, F., and Ulm, R. (2014). UV-B-responsive association of the Arabidopsis bZIP transcription factor ELONGATED HYPOCOTYL5 with target genes, including its own promoter. Plant Cell **26:** 4200–4213.

Boch, J. (2011). TALEs of genome targeting. Nat. Biotechnol. **29:** 135–136.

Bonente, G., Passarini, F., Cazzaniga, S., Mancone, C., Buia, M.C., Tripodi, M., Bassi, R., and Caffarri, S. (2008). The occurrence of the *psbS* gene product in *Chlamydomonas reinhardtii* and in other photosynthetic organisms and its correlation with energy quenching. Photochem. Photobiol. **84:** 1359–1370.

Booij-James, I.S., Dube, S.K., Jansen, M.A.K., Edelman, M., and Mattoo, A.K. (2000). Ultraviolet-B radiation impacts light-mediated turnover of the photosystem II reaction center heterodimer in Arabidopsis mutants altered in phenolic metabolism. Plant Physiol. **124:** 1275–1284.

Boudreau, E., Nickelsen, J., Lemaire, S.D., Ossenbühl, F., and Rochaix, J.D. (2000). The *Nac2* gene of Chlamydomonas encodes a chloroplast TPR-like protein involved in *psbD* mRNA stability. EMBO J. **19:** 3366–3376.

Brown, B.A., and Jenkins, G.I. (2008). UV-B signaling pathways with different fluence-rate response profiles are distinguished in mature Arabidopsis leaf tissue by requirement for UVR8, HY5, and HYH. Plant Physiol. **146:** 576–588.

Brown, B.A., Cloix, C., Jiang, G.H., Kaiserli, E., Herzyk, P., Kliebenstein, D.J., and Jenkins, G.I. (2005). A UV-B-specific signaling component orchestrates plant UV protection. Proc. Natl. Acad. Sci. USA **102:** 18225–18230.

Chaturvedi, R., and Shyam, R. (2000). Degradation and de novo synthesis of D1 protein and psbA transcript levels in *Chlamydomonas reinhardtii* during UV-B inactivation of photosynthesis and its reactivation. J. Biosci. **25:** 65–71.

Christie, J.M., Arvai, A.S., Baxter, K.J., Heilmann, M., Pratt, A.J., O'Hara, A., Kelly, S.M., Hothorn, M., Smith, B.O., Hitomi, K., Jenkins, G.I., and Getzoff, E.D. (2012). Plant UVR8 photoreceptor senses UV-B by tryptophan-mediated disruption of cross-dimer salt bridges. Science **335:** 1492–1496.

Cloix, C., Kaiserli, E., Heilmann, M., Baxter, K.J., Brown, B.A., O'Hara, A., Smith, B.O., Christie, J.M., and Jenkins, G.I. (2012). C-terminal region of the UV-B photoreceptor UVR8 initiates signaling through interaction with the COP1 protein. Proc. Natl. Acad. Sci. USA **109:** 16366–16370.

Clough, S.J., and Bent, A.F. (1998). Floral dip: a simplified method for Agrobacterium-mediated transformation of *Arabidopsis thaliana*. Plant J. **16:** 735–743.

Davey, M.P., Susanti, N.I., Wargent, J.J., Findlay, J.E., Paul Quick, W., Paul, N.D., and Jenkins, G.I. (2012). The UV-B photoreceptor UVR8 promotes photosynthetic efficiency in *Arabidopsis thaliana* exposed to elevated levels of UV-B. Photosynth. Res. **114:** 121–131.

Depège, N., Bellafiore, S., and Rochaix, J.D. (2003). Role of chloroplast protein kinase Stt7 in LHCII phosphorylation and state transition in Chlamydomonas. Science **299:** 1572–1575.

Dobrikova, A.G., and Apostolova, E.L. (2015). Damage and protection of the photosynthetic apparatus from UV-B radiation. II. Effect of quercetin at different pH. J. Plant Physiol. **184:** 98–105.

Duanmu, D., Casero, D., Dent, R.M., Gallaher, S., Yang, W., Rockwell, N.C., Martin, S.S., Pellegrini, M., Niyogi, K.K., Merchant, S.S., Grossman, A.R., and Lagarias, J.C. (2013). Retrograde bilin signaling enables Chlamydomonas greening and phototrophic survival. Proc. Natl. Acad. Sci. USA **110:** 3621–3626.

Edgar, R., Domrachev, M., and Lash, A.E. (2002). Gene Expression Omnibus: NCBI gene expression and hybridization array data repository. Nucleic Acids Res. **30:** 207–210.

Favory, J.J., et al. (2009). Interaction of COP1 and UVR8 regulates UV-B-induced photomorphogenesis and stress acclimation in Arabidopsis. EMBO J. **28:** 591–601.

González Besteiro, M.A., Bartels, S., Albert, A., and Ulm, R. (2011). Arabidopsis MAP kinase phosphatase 1 and its target MAP kinases 3 and 6 antagonistically determine UV-B stress tolerance, independent of the UVR8 photoreceptor pathway. Plant J. **68:** 727–737.

Gorman, D.S., and Levine, R.P. (1965). Cytochrome f and plastocyanin: their sequence in the photosynthetic electron transport chain of *Chlamydomonas reinhardi.* Proc. Natl. Acad. Sci. USA **54:** 1665–1669.

Gruber, H., Heijde, M., Heller, W., Albert, A., Seidlitz, H.K., and Ulm, R. (2010). Negative feedback regulation of UV-B-induced photomorphogenesis and stress acclimation in Arabidopsis. Proc. Natl. Acad. Sci. USA **107:** 20132–20137.

Gutman, B.L., and Niyogi, K.K. (2004). Chlamydomonas and Arabidopsis. A dynamic duo. Plant Physiol. **135:** 607–610.

Hader, D.P. (2000). Effects of solar UV-B radiation on aquatic ecosystems. Adv. Space Res. **26:** 2029–2040.

Hakala-Yatkin, M., Mäntysaari, M., Mattila, H., and Tyystjärvi, E. (2010). Contributions of visible and ultraviolet parts of sunlight to photoinhibition. Plant Cell Physiol. **51:** 1745–1753.

Harris, E.H. (2009). The Chlamydomonas Sourcebook. (San Diego, CA: Academic Press).

Heijde, M., and Ulm, R. (2012). UV-B photoreceptor-mediated signalling in plants. Trends Plant Sci. **17:** 230–237.

Heijde, M., and Ulm, R. (2013). Reversion of the Arabidopsis UV-B photoreceptor UVR8 to the homodimeric ground state. Proc. Natl. Acad. Sci. USA **110:** 1113–1118.

Heijde, M., Binkert, M., Yin, R., Ares-Orpel, F., Rizzini, L., Van De Slijke, E., Persiau, G., Nolf, J., Gevaert, K., De Jaeger, G., and Ulm, R. (2013). Constitutively active UVR8 photoreceptor variant in Arabidopsis. Proc. Natl. Acad. Sci. USA **110:** 20326–20331.

Heilmann, M., and Jenkins, G.I. (2013). Rapid reversion from monomer to dimer regenerates the ultraviolet-B photoreceptor UV RESISTANCE LOCUS8 in intact Arabidopsis plants. Plant Physiol. **161:** 547–555.

Huang, K., and Beck, C.F. (2003). Phototropin is the blue-light receptor that controls multiple steps in the sexual life cycle of the green alga *Chlamydomonas reinhardtii.* Proc. Natl. Acad. Sci. USA **100:** 6269–6274.

Huang, X., Yang, P., Ouyang, X., Chen, L., and Deng, X.W. (2014). Photoactivated UVR8-COP1 module determines photomorphogenic UV-B signaling output in Arabidopsis. PLoS Genet. **10:** e1004218.

Jansen, M.A.K., Gaba, V., Greenberg, B.M., Mattoo, A.K., and Edelman, M. (1996). Low threshold levels of ultraviolet-B in a background of photosynthetically active radiation trigger rapid degradation of the D2 protein of photosystem-II. Plant J. **9:** 693–699.

Järvi, S., Suorsa, M., and Aro, E.-M. (2015). Photosystem II repair in plant chloroplasts–Regulation, assisting proteins and shared components with photosystem II biogenesis. Biochim. Biophys. Acta **1847:** 900–909.

Jenkins, G.I. (2014). The UV-B photoreceptor UVR8: from structure to physiology. Plant Cell **26:** 21–37.

Karimi, M., Inzé, D., and Depicker, A. (2002). GATEWAY vectors for Agrobacterium-mediated plant transformation. Trends Plant Sci. **7:** 193–195.

Kateriya, S., Nagel, G., Bamberg, E., and Hegemann, P. (2004). "Vision" in single-celled algae. News Physiol. Sci. **19:** 133–137.

Kianianmomeni, A., and Hallmann, A. (2014). Algal photoreceptors: in vivo functions and potential applications. Planta **239:** 1–26.

Kliebenstein, D.J., Lim, J.E., Landry, L.G., and Last, R.L. (2002). Arabidopsis UVR8 regulates ultraviolet-B signal transduction and tolerance and contains sequence similarity to human regulator of chromatin condensation 1. Plant Physiol. **130:** 234–243.

Kropat, J., Hong-Hermesdorf, A., Casero, D., Ent, P., Castruita, M., Pellegrini, M., Merchant, S.S., and Malasarn, D. (2011). A revised mineral nutrient supplement increases biomass and growth rate in *Chlamydomonas reinhardtii.* Plant J. **66:** 770–780.

Kuras, R., Saint-Marcoux, D., Wollman, F.A., and de Vitry, C. (2007). A specific c-type cytochrome maturation system is required for oxygenic photosynthesis. Proc. Natl. Acad. Sci. USA **104:** 9906–9910.

Li, J., Yang, L., Jin, D., Nezames, C.D., Terzaghi, W., and Deng, X.W. (2013). UV-B-induced photomorphogenesis in Arabidopsis. Protein Cell **4:** 485–492.

Luck, M., Mathes, T., Bruun, S., Fudim, R., Hagedorn, R., Tran Nguyen, T.M., Kateriya, S., Kennis, J.T.M., Hildebrandt, P., and Hegemann, P. (2012). A photochromic histidine kinase rhodopsin (HKR1) that is bimodally switched by ultraviolet and blue light. J. Biol. Chem. **287:** 40083–40090.

Mathes, T., Heilmann, M., Pandit, A., Zhu, J., Ravensbergen, J., Kloz, M., Fu, Y., Smith, B.O., Christie, J.M., Jenkins, G.I., and Kennis, J.T. (2015). Proton-coupled electron transfer constitutes the photoactivation mechanism of the plant photoreceptor UVR8. J. Am. Chem. Soc. **137:** 8113–8120.

Merchant, S.S., et al. (2007). The Chlamydomonas genome reveals the evolution of key animal and plant functions. Science **318:** 245–250.

Molnar, A., Bassett, A., Thuenemann, E., Schwach, F., Karkare, S., Ossowski, S., Weigel, D., and Baulcombe, D. (2009). Highly specific gene silencing by artificial microRNAs in the unicellular alga *Chlamydomonas reinhardtii.* Plant J. **58:** 165–174.

Nagel, G., Ollig, D., Fuhrmann, M., Kateriya, S., Musti, A.M., Bamberg, E., and Hegemann, P. (2002). Channelrhodopsin-1: a light-gated proton channel in green algae. Science **296:** 2395–2398.

Nagel, G., Szellas, T., Huhn, W., Kateriya, S., Adeishvili, N., Berthold, P., Ollig, D., Hegemann, P., and Bamberg, E. (2003). Channelrhodopsin-2, a directly light-gated cation-selective membrane channel. Proc. Natl. Acad. Sci. USA **100:** 13940–13945.

Niyogi, K.K., and Truong, T.B. (2013). Evolution of flexible nonphotochemical quenching mechanisms that regulate light harvesting in oxygenic photosynthesis. Curr. Opin. Plant Biol. **16:** 307–314.

O'Hara, A., and Jenkins, G.I. (2012). In vivo function of tryptophans in the Arabidopsis UV-B photoreceptor UVR8. Plant Cell **24:** 3755–3766.

Oravecz, A., Baumann, A., Máté, Z., Brzezinska, A., Molinier, J., Oakeley, E.J., Ádám, E., Schäfer, E., Nagy, F., and Ulm, R. (2006). CONSTITUTIVELY PHOTOMORPHOGENIC1 is required for the UV-B response in Arabidopsis. Plant Cell **18:** 1975–1990.

Peers, G., Truong, T.B., Ostendorf, E., Busch, A., Elrad, D., Grossman, A.R., Hippler, M., and Niyogi, K.K. (2009). An ancient light-harvesting protein is critical for the regulation of algal photosynthesis. Nature **462:** 518–521.

Peng, J., and Xu, J. (2011). RaptorX: exploiting structure information for protein alignment by statistical inference. Proteins **79** (suppl. 10): 161–171.

Ranjan, A., Dickopf, S., Ullrich, K.K., Rensing, S.A., and Hoecker, U. (2014). Functional analysis of COP1 and SPA orthologs from Physcomitrella and rice during photomorphogenesis of transgenic Arabidopsis reveals distinct evolutionary conservation. BMC Plant Biol. **14:** 178.

Reisdorph, N.A., and Small, G.D. (2004). The *CPH1* gene of *Chlamydomonas reinhardtii* encodes two forms of cryptochrome whose levels are controlled by light-induced proteolysis. Plant Physiol. **134:** 1546–1554.

Richter, P., Helbling, W., Streb, C., and Häder, D.P. (2007). PAR and UV effects on vertical migration and photosynthesis in *Euglena gracilis.* Photochem. Photobiol. **83:** 818–823.

Rizzini, L., Favory, J.J., Cloix, C., Faggionato, D., O'Hara, A., Kaiserli, E., Baumeister, R., Schäfer, E., Nagy, F., Jenkins, G.I., and Ulm, R. (2011). Perception of UV-B by the Arabidopsis UVR8 protein. Science **332:** 103–106.

Robinson, M.D., McCarthy, D.J., and Smyth, G.K. (2010). edgeR: a Bioconductor package for differential expression analysis of digital gene expression data. Bioinformatics **26:** 139–140.

Rochaix, J.D. (2002). Chlamydomonas, a model system for studying the assembly and dynamics of photosynthetic complexes. FEBS Lett. **529:** 34–38.

Rozema, J., van de Staaij, J., Björn, L.O., and Caldwell, M. (1997). UV-B as an environmental factor in plant life: stress and regulation. Trends Ecol. Evol. (Amst.) **12:** 22–28.

Schierenbeck, L., Ries, D., Rogge, K., Grewe, S., Weisshaar, B., and Kruse, O. (2015). Fast forward genetics to identify mutations causing a high light tolerant phenotype in *Chlamydomonas reinhardtii* by whole-genome-sequencing. BMC Genomics **16:** 57.

Schuster, G., Timberg, R., and Ohad, I. (1988). Turnover of thylakoid photosystem II proteins during photoinhibition of *Chlamydomonas reinhardtii.* Eur. J. Biochem. **177:** 403–410.

Shimogawara, K., Fujiwara, S., Grossman, A., and Usuda, H. (1998). High-efficiency transformation of *Chlamydomonas reinhardtii* by electroporation. Genetics **148:** 1821–1828.

Stracke, R., Favory, J.J., Gruber, H., Bartelniewoehner, L., Bartels, S., Binkert, M., Funk, M., Weisshaar, B., and Ulm, R. (2010). The Arabidopsis bZIP transcription factor HY5 regulates expression of the *PFG1/MYB12* gene in response to light and ultraviolet-B radiation. Plant Cell Environ. **33:** 88–103.

Takahashi, S., and Badger, M.R. (2011). Photoprotection in plants: a new light on photosystem II damage. Trends Plant Sci. **16:** 53–60.

Takahashi, S., Milward, S.E., Yamori, W., Evans, J.R., Hillier, W., and Badger, M.R. (2010). The solar action spectrum of photosystem II damage. Plant Physiol. **153:** 988–993.

Tilbrook, K., Arongaus, A.B., Binkert, M., Heijde, M., Yin, R., and Ulm, R. (2013). The UVR8 UV-B photoreceptor: perception, signaling and response. Arabidopsis Book **11:** e0164.

Trapnell, C., Pachter, L., and Salzberg, S.L. (2009). TopHat: discovering splice junctions with RNA-Seq. Bioinformatics **25:** 1105–1111.

Ulm, R., Baumann, A., Oravecz, A., Máté, Z., Adám, E., Oakeley, E.J., Schäfer, E., and Nagy, F. (2004). Genome-wide analysis of gene expression reveals function of the bZIP transcription factor HY5 in the UV-B response of Arabidopsis. Proc. Natl. Acad. Sci. USA **101:** 1397–1402.

Vandenbussche, F., Tilbrook, K., Fierro, A.C., Marchal, K., Poelman, D., Van Der Straeten, D., and Ulm, R. (2014). Photoreceptor-mediated bending towards UV-B in Arabidopsis. Mol. Plant **7:** 1041–1052.

Wargent, J.J., Elfadly, E.M., Moore, J.P., and Paul, N.D. (2011). Increased exposure to UV-B radiation during early development leads to enhanced photoprotection and improved long-term performance in *Lactuca sativa.* Plant Cell Environ. **34:** 1401–1413.

Wargent, J.J., Nelson, B.C., McGhie, T.K., and Barnes, P.W. (2015). Acclimation to UV-B radiation and visible light in *Lactuca sativa* involves up-regulation of photosynthetic performance and orchestration of metabolome-wide responses. Plant Cell Environ. **38:** 929–940.

Wu, D., Hu, Q., Yan, Z., Chen, W., Yan, C., Huang, X., Zhang, J., Yang, P., Deng, H., Wang, J., Deng, X., and Shi, Y. (2012). Structural basis of ultraviolet-B perception by UVR8. Nature **484:** 214–219.

Wu, H., Abasova, L., Cheregi, O., Deák, Z., Gao, K., and Vass, I. (2011). D1 protein turnover is involved in protection of Photosystem II against UV-B induced damage in the cyanobacterium *Arthrospira* (*Spirulina*) *platensis.* J. Photochem. Photobiol. B **104:** 320–325.

Yi, C., and Deng, X.W. (2005). COP1 - from plant photomorphogenesis to mammalian tumorigenesis. Trends Cell Biol. **15:** 618–625.

Yin, R., Arongaus, A.B., Binkert, M., and Ulm, R. (2015). Two distinct domains of the UVR8 photoreceptor interact with COP1 to initiate UV-B signaling in Arabidopsis. Plant Cell **27:** 202–213.

Zeng, X., Ren, Z., Wu, Q., Fan, J., Peng, P.-P., Tang, K., Zhang, R., Zhao, K.-H., and Yang, X. (2015). Dynamic crystallography reveals early signalling events in ultraviolet photoreceptor UVR8. Nat. Plants **1:** 14006.

Zhang, Y. (2008). I-TASSER server for protein 3D structure prediction. BMC Bioinformatics **9:** 40.